

**TOTAL SKIN  
ELECTRON THERAPY:  
TECHNIQUE AND DOSIMETRY**



**AAPM REPORT NO. 23**

**TOTAL SKIN  
ELECTRON THERAPY:  
TECHNIQUE AND DOSIMETRY**

**REPORT OF TASK GROUP 30  
RADIATION THERAPY COMMITTEE  
AAPM**

C. J. Karzmark, Ph.D., Chairman  
Therapeutic Radiology Department  
Stanford University School of Medicine  
Stanford, California 94305

**Members**

Joseph Anderson  
Alfonso Buffa

Peter Fessenden  
Faiz Khan

Goran Svensson  
Kenneth Wright

**Consultants**

Peter Almond  
Benedick Fraass

Kenneth Hogstrom  
Robert Loevinger

Robert Morton  
Bernice Palos

**Other Contributors**

Peter Biggs  
Edgar Dally  
Stan Johnsen

Pat Johnson  
Mark Kao  
Ravi Nath

Craig Nunan  
Ervin Podgorsak  
Chester Reft

December 1987

Published for the  
American Association of Physicists in Medicine  
by the American Institute of Physics

Further copies of this report may be obtained from

Executive Officer  
American Association of Physicists in Medicine  
335 E. 45 Street  
New York, NY 10017

Library of Congress Catalog Card Number: 88-70047  
International Standard Book Number: 0-88318-556-3  
International Standard Serial Number: 0271-7344

Copyright © 1988 by the American Association  
of Physicists in Medicine

All rights reserved. No part of this publication may be reproduced, stored in a retrieval system, or transmitted in any form or by any means (electronic, mechanical, photocopying, recording, or otherwise) without the prior written permission of the publisher.

Published by the American Institute of Physics, Inc.,  
335 East 45 Street, New York, New York 10017

Printed in the United States of America

TOTAL SKIN ELECTRON THERAPY: TECHNIQUE AND DOSIMETRY

TABLE OF CONTENTS

1.	INTRODUCTION	
2.	IRRADIATION REQUIREMENTS	4
	2.1 Irradiation beam requirements	4
	2.2 Irradiation room requirements	13
3.	IRRADIATION TECHNIQUES	14
	3.1 Beta particles	16
	3.2 Narrow rectangular beam	16
	3.3 Scattered single beam	17
	3.4 Pair of parallel beams	18
	3.5 Pair of angled beams	18
	3.6 Pendulum-arc	19
	3.7 Patient rotation	19
4.	SIX DUAL-FIELD IRRADIATION TECHNIQUE	20
	4.1 Irradiation geometry	20
	4.2 Beam characteristics at treatment plane	20
	4.2.1 Single horizontal beam	20
	4.2.2 Dual-field beams	23
	4.2.3 Six dual-field beams	25
5.	LINAC OPERATING CONDITIONS	25
	5.1 Linac operating parameters	25
	5.2 Beam scatterer-energy degraders	27
	5.3 Beam monitoring	29
6.	DOSIMETRY AND INSTRUMENTATION	32
	6.1 Dosimetry methods	32
	6.2 Dosimetry phantoms	33
	6.3 Dosimetry measurements	34
	6.4 Multiple-field measurements	37
	6.5 Calibration point dose measurements	38
	6.6 Treatment skin dose measurements	38
	6.7 Precautions and routine checks	39
7.	PATIENT CONSIDERATIONS	40
	7.1 Patient positioning	40
	7.2 Patient support devices	41

7.3 Patient shielding	43
7.4 Local boost fields	44
7.5 In-vivo dose measurement	45
Table I Physical considerations	47
Table II Example treatment prescription	47
Table III Example changeover procedure	47
8. BIBLIOGRAPHY	48

## 1. INTRODUCTION

This report describes the techniques and dosimetry for Total Skin Electron Therapy (TSET) at energies of about 3-7 MeV at the patient and 4-10 MeV at the accelerator beam-exit window. The irradiation beam requirements are identified on the basis of clinical needs for the treatment of cutaneous T-cell lymphoma, a chronic progressive lymphoma, most often treated with TSET. It is usually called mycosis fungoides, but is sometimes denoted as Sezary syndrome. This therapy is also identified in the literature by combinations of words in part abstracted from TSET together with additions such as: whole body or whole skin, superficial irradiation, or electron beam. The title Total Skin Electron Beam Therapy (TSEBT) is such an example.

Methods of obtaining the very large fields needed for electron beam irradiation of the total skin are reviewed. Recommendations are made regarding the types of dosimetric measurements that should be performed prior to initiating such irradiation procedures. One widely used technique for TSET, which involves six dual fields, is described thoroughly and others are reviewed briefly. It is expected that the technically experienced reader will develop sufficient understanding from reading this report, and pertinent references, to implement the treatment techniques described herein. The report is written primarily for the medical radiological physicists who might wish to develop a TSET program at their own facility at the request of the radiation oncologist.

It is acknowledged that any TSET program development is heavily dependent on the specific technique chosen, the particular equipment on which it is carried out and the facility where it will be implemented. The techniques themselves are often complex with concomitant hazards and most are time consuming to develop and carry out on a routine basis. A rigorous quality assurance program should be an integral part of a TSET program, particularly because high electron dose rates at isocenter are usually employed to minimize treatment time in a plane several meters distant. This entails operating the accelerator at beam currents greater than those required for small-field, 100 cm SSD electron treatments and comparable to those used in X-ray therapy. This results in a high electron dose rate at isocenter and necessitates special attention to safety measures such as interlocks, beam monitoring, etc. Whether a physicist should be present for TSET treatments depends on the complexity of the procedure and the relevant staff's experience in using it. These considerations, together with the relatively small mycosis fungoides patient population, suggest that the TSET modality be confined to a small number of centers with due consideration of regional needs. Most patients are between 45 and 69 years of age at diagnosis, but the disease may occur at any age, including childhood. In the United States, the average yearly

incidence rate of mycosis fungoides in the 45 to 69 year range is roughly 3 per  $10^6$  people.<sup>32, 97</sup>

The subject of TSET is introduced in Section 1. The irradiation beam and room requirements for TSET are described in Section 2. The various irradiation techniques are outlined in Section 3. The irradiation geometry and electron beam characteristics for single and dual angled fields are described in detail for the widely used combination of six dual fields in Section 4. Emphasis is placed on treatment with electron linacs, which are frequently employed for this treatment modality. Section 5 is devoted to linac operating conditions applicable to TSET, and Section 6 covers dosimetry and instrumentation. Specific physical considerations concerning individual patients are covered in Section 7. A comprehensive bibliography is provided in Section 8. The various physical considerations involved in a TSET program are summarized in Table I. Table II provides a representative TSET treatment prescription and Table III outlines the treatment unit changeover procedure employed in going from X-ray therapy to TSET.

## 2. IRRADIATION REQUIREMENTS

### 2.1 Irradiation beam requirements

The irradiation beam requirements involve characteristics of the treatment electron beam, the disease entity and the patient population. They include specification of: field size, penetration, energy, dose, dose rate, field flatness in the treatment plane, X-ray background, and the need for and nature of boost fields. A standing patient is assumed unless noted otherwise since most treatment techniques involve this patient position. The central requirement is to treat virtually the entire body surface to a limited depth and to a uniform dose using electrons with a low X-ray background. These requirements coupled with the varied obliquity of body surfaces and beam directions, patient self-shielding, etc., combine in a complex manner to produce a dose distribution less uniform than desirable and significantly less uniform than for conventional small-field electron treatment modalities. The geometry of the treatment technique is shown in Fig. 1.

The field size of the composite electron beam at the patient treatment plane must be approximately 200 cm in height by 80 cm in width to encompass the largest patient. Within this rectangle, a vertical uniformity of  $\pm 8\%$  and a horizontal uniformity of  $\pm 4\%$  over the central 160 cm x 60 cm area of the treatment plane are achievable goals for most techniques. The uniformity of dose achieved in phantom studies in the treatment plane cannot be reproduced over the patient. Kumar et al., for example,, found that a  $\pm 7.5\%$  variation in the treatment plane may increase to  $\pm 15\%$  at the patient due to variable skin distance, self shielding, and patient motion except in the perineal region where the dose may

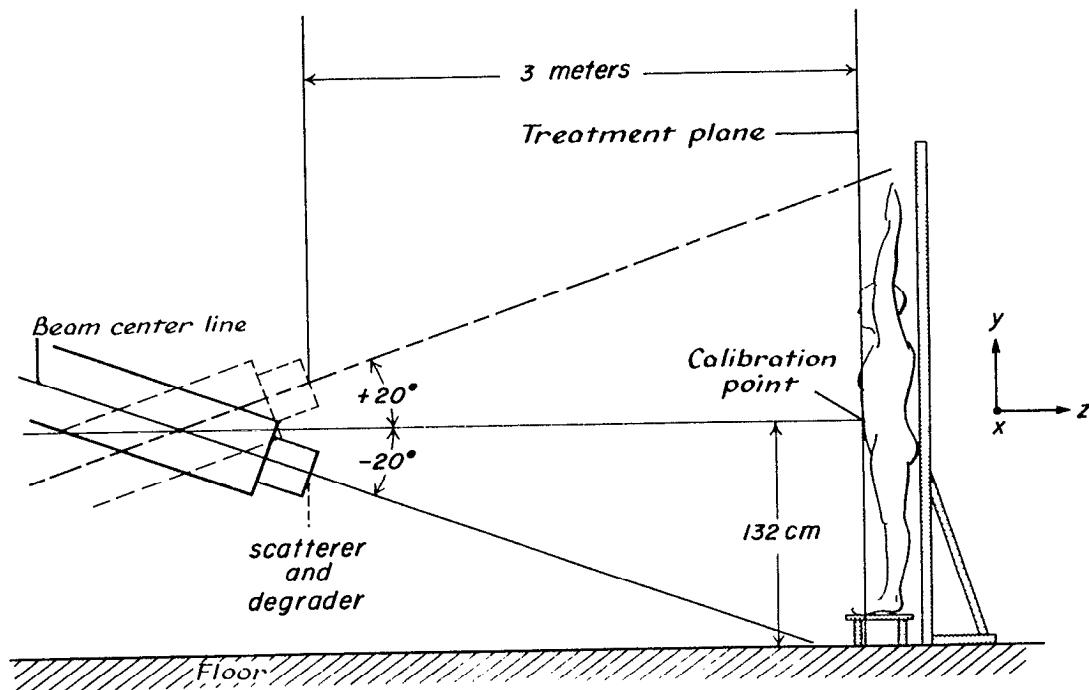


Fig. 1a. Geometrical arrangement of the symmetrical dual-field treatment technique. Equal exposures are given with each beam. The calibration point dose is at  $(x=0, y=0)$  in the treatment plane.



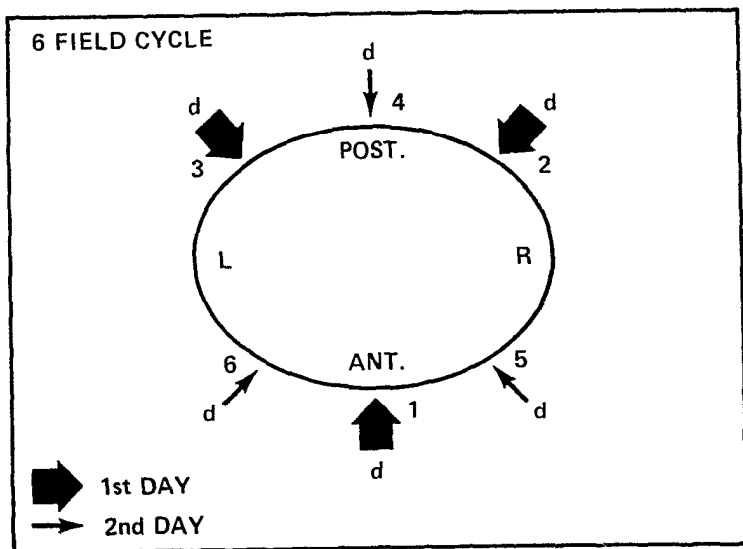


Fig. 1b. Sequential two-day treatment cycle illustrating the angular orientation of the six dual-fields.

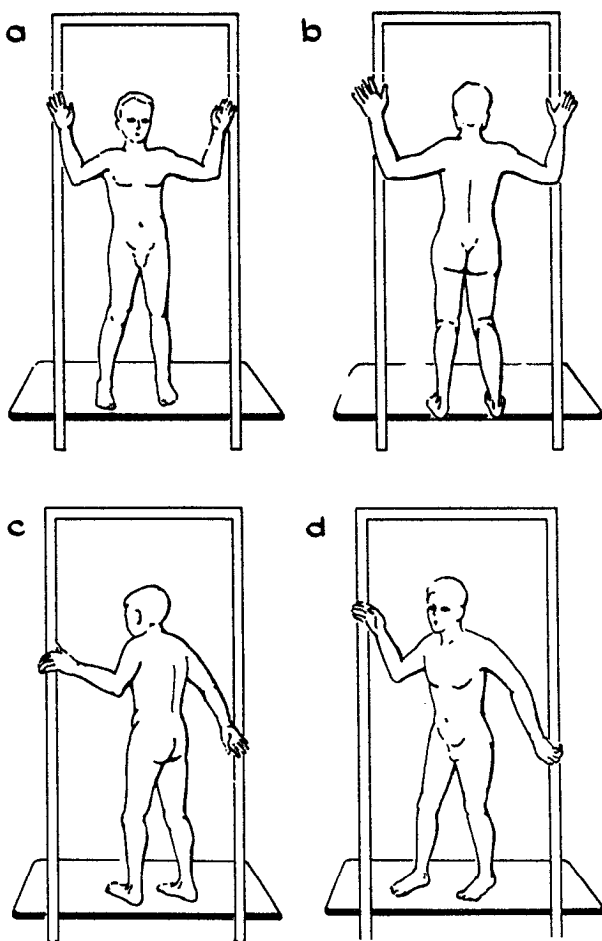


Fig. 1c. Patient position stances for the anterior, posterior, and two of the angled dual-field exposures.

fall to 30 to 40% of the prescribed value.<sup>69,70</sup>

The requisite penetration depth is usually thought to vary with the stage and type of disease and may vary over the body surface.<sup>7,45</sup> A penetration depth range from approximately 5 mm to 15 mm or more at the 50% isodose surface encompasses most lesions. It appears advantageous to provide more than one TSET beam energy to cover this range of depths. Since many electrons enter body surfaces obliquely, the energy required at the patient treatment plane for a specified average penetration depth is significantly greater than that obtained from invoking the simplistic energy loss approximation of  $2 \text{ MeV}/(\text{g}/\text{cm}^2)$ .

The electron beam incident on the exit window of the accelerator can be characterized by a relatively narrow distribution of energy fluence whose peak is termed the accelerator energy,  $E_a$ . This parameter and others employed to characterize various electron beam energies are illustrated in Fig. 2. As the beam passes through the exit window and different materials between the exit window and the phantom surface, the energy will decrease and the energy spread will increase. The energy fluence distribution of such a beam arriving at the treatment plane (phantom surface) is characterized by its peak, or most probable energy  $E_{p,o}$ , and a lower mean energy  $\bar{E}_o$ . The value of  $E_{p,o}$  can be obtained by subtracting the most probable energy loss in the energy-degrading materials traversed from the accelerator energy  $E_a$ , or from the range-energy equation given below. In this low energy range, the most probable energy loss for the low-energy TSET electrons is just the mean collision ionization energy loss for an electron of energy  $E_a$ .

The range-energy relationship:

$$E_{p,o} = 1.95R_p + 0.48$$

is used to relate the most probable energy at the phantom surface,  $E_{p,o}$  in MeV, to the practical range,  $R_p$  in cm of water.<sup>53</sup> The mean energy at the phantom surface (treatment plane),  $\bar{E}_o$  in MeV is related to the half-value depth  $R_{50}$  in cm of water by:<sup>51,53</sup>

$$\bar{E}_o = 2.33 R_{50}$$

Illustrations of  $R_p$  and  $R_{50}$  are given in Fig. 3. The treatment beam traversing the patient or phantom further degrades and spreads out in energy. Its mean energy can be estimated as a function of depth  $z$  and the mean entrance energy  $\bar{E}_o$  by the equation:

$$\bar{E}_z = \bar{E}_o (1 - z/R_p)$$

As noted earlier, the incident mean electron beam energy  $\bar{E}_o$  at the patient treatment plane is usually in the range 3 to 7 MeV

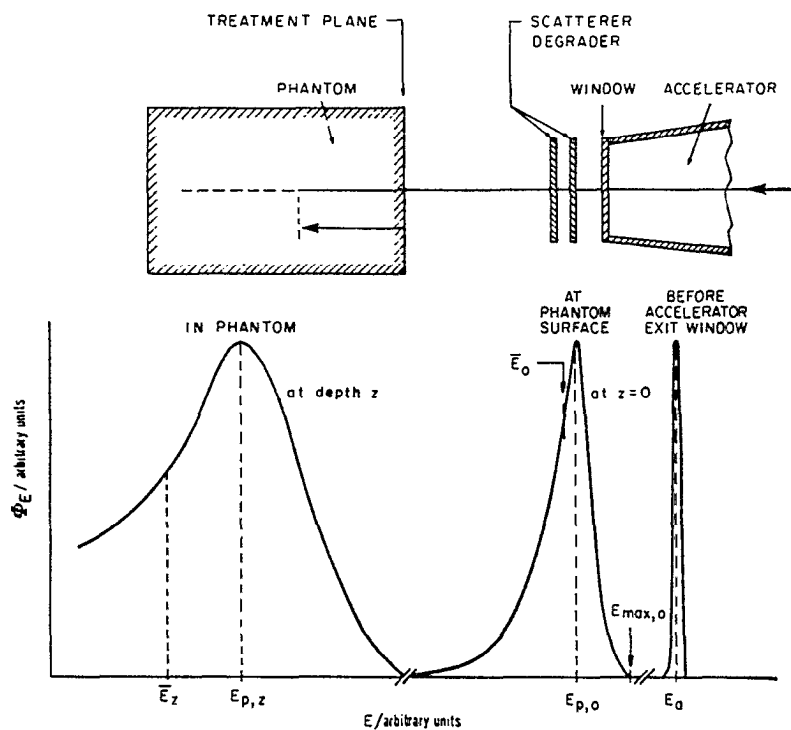


Fig. 2. Energy parameters used to characterize an electron therapy beam. The ordinate is electron fluence in arbitrary units.

## DEPTH IONIZATION FOR LARGE FIELD ELECTRON TREATMENT

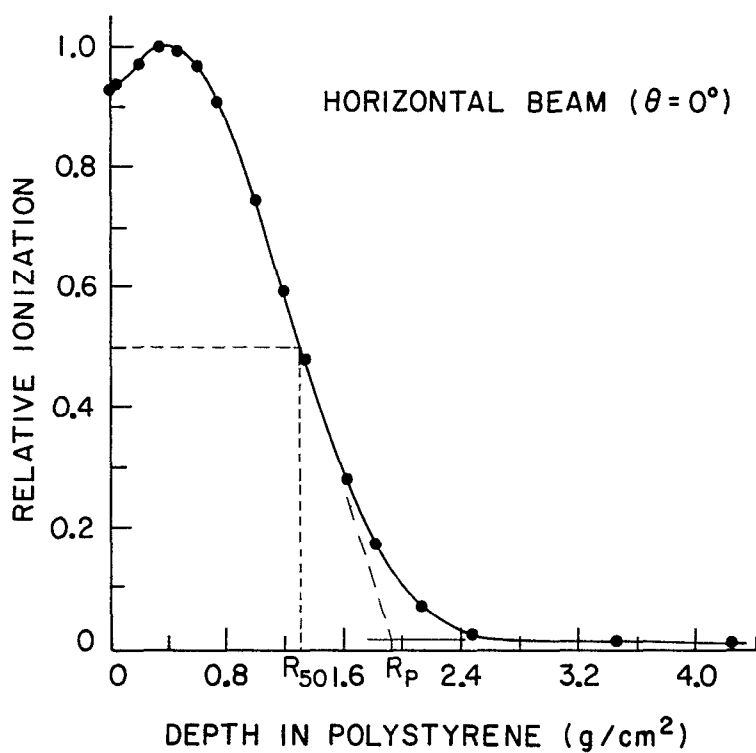


Fig. 3a. Central axis depth-ionization curve in polystyrene. The measurements were made with a single horizontal beam directed at point (0,0) in the treatment plane using a parallel-plate ionization chamber.

# DEPTH DOSE FOR LARGE FIELD ELECTRON TREATMENT WITH $\theta = \pm 20^\circ$

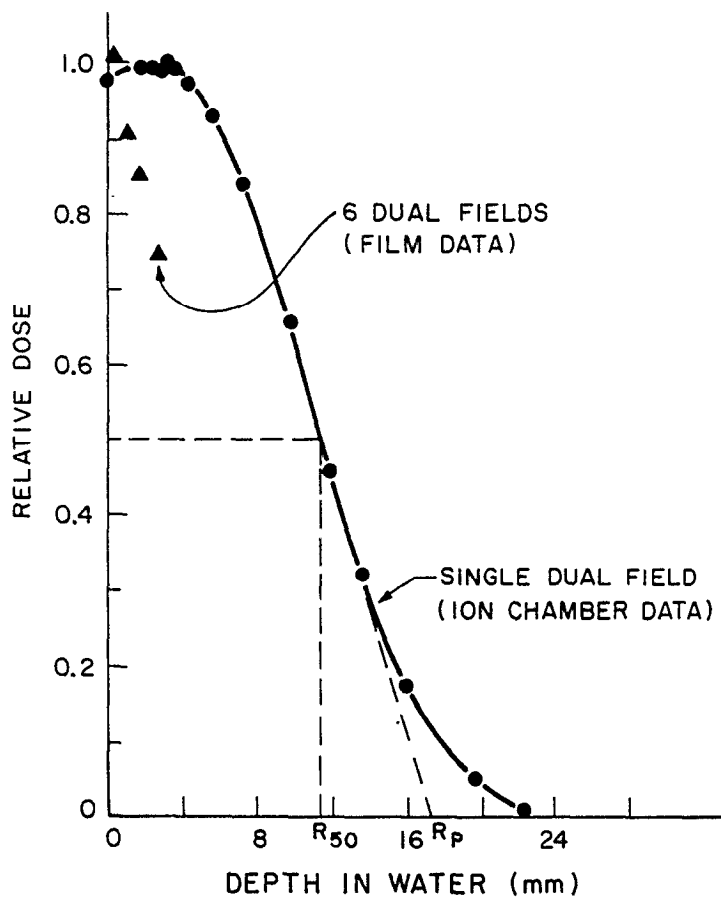


Fig. 3b. Relative depth dose in water for a single  $\pm 20^\circ$  dual-field exposure for the same accelerator energy as in Fig. 3a.

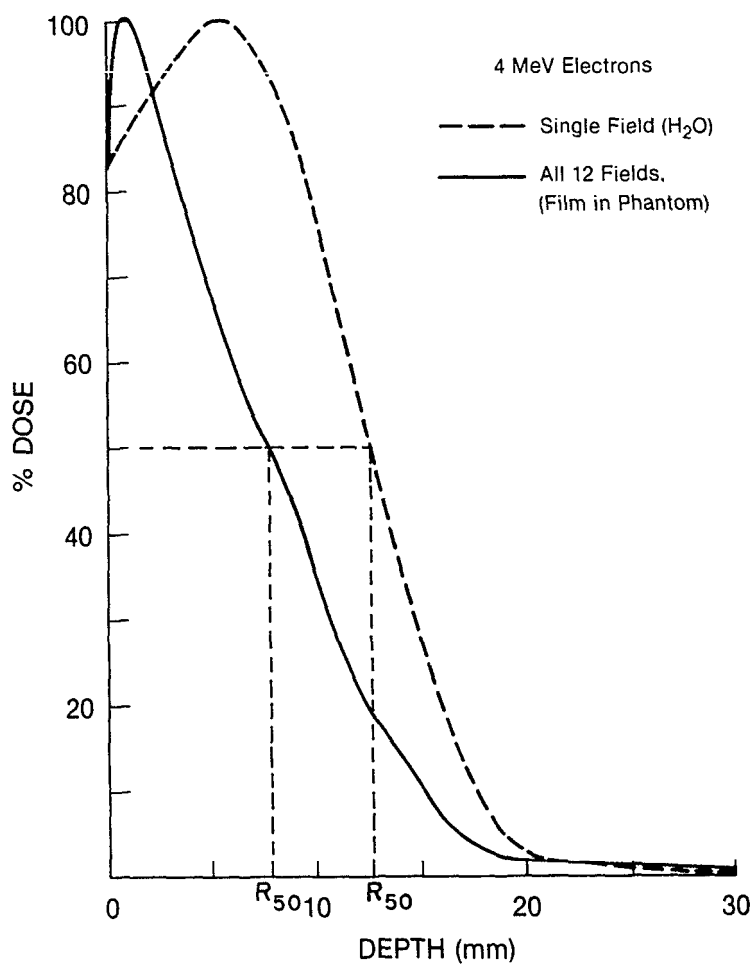


Fig. 3c. Depth doses in water for a single field with  $\theta = 0$  and for all 12 fields (six dual fields) using film in a humanoid phantom (Fraass<sup>27</sup>).

with accelerator energies,  $E_e$ , ranging from about 4 to 10 MeV. Occasionally, lower energies have been employed. Most irradiation techniques involve significant electron energy loss from the sequence of materials traversed by the electron beam, as much as several MeV between the accelerator vacuum and the patient treatment plane.

Often, there are body areas shielded in part by other body sections or inadequately exposed because of limitations of the geometry of the treatment technique. Small supplementary boost fields of electrons or orthovoltage X-rays are therefore frequently needed.

The accompanying megavoltage X-ray background is penetrating and forward directed; it often exposes much of the body volume and should be as low as reasonably achievable. It is roughly proportional to the number of fields used since all fields contribute penetrating X-rays; often it can be estimated prior to the selection of the technique. The average X-ray dose can be reduced by angling the beam axes so that the peaks of the forward-directed X-rays lie outside the body. A desirable X-ray background level averaged over the body volume is 1% or less of the total mean electron dose at dose maximum. This may be difficult to achieve with some equipment and techniques. A representative treatment prescription shown in Table II of 36 Gy in nine weeks (given four days per week by three dual fields per day [Fig. 1] averaging 1 Gy per treatment day) would give an average total dose to the skin of 36 Gy for a 1% X-ray contamination of 0.36 Gy.

Most TSET procedures are time-consuming to carry out because of the multiple field and patient-position requirements. Since patients requiring TSET are often elderly and infirm, a high dose rate, which shortens the treatment time, is desirable. Average dose rates from 0.25 to several grays per minute at the depth of dose maximum are used, with the lower end of this range usually considered only marginally acceptable. Some patients require physical support devices to ensure their safety as well as correct positioning in a standing position. Radiation shielding of specific anatomical surfaces or organs may also be required. Commonly, finger and toe nails, tops of feet, and the eyes are protected during at least part of the treatment, with the use of shielding being dependent on the extent of disease.

## 2.2 Irradiation room requirements

Providing good dose uniformity over the height and width of a patient usually necessitates the use of large distances between scatterer and patient, typically 2-7 meters, with the distance being technique dependent. Hence, existing treatment room layouts may restrict the choice of a TSET technique.

The TSET procedure involves significant ozone production from



ionizing large volumes of air in the treatment room. Frequent exchange of the air in the treatment room is essential for confining ozone exposure to acceptable limits. Ozone concentration in the treatment room should be evaluated by a qualified health physicist.

For most installations, the shielding provided by megavoltage X-ray treatment rooms has been found adequate for TSET therapy which involves bringing a large fluence of energetic electrons out into the treatment room. However, measurements must be made to ensure that radiation protection for TSET is adequate. Note should be taken of the range in air of electrons, the widespread scattering of electrons and bremsstrahlung production<sup>18, 82</sup> when the electrons are not stopped in the patient or other low-Z material. Megavoltage electrons have a maximum range of about 0.5 g/cm<sup>2</sup> per MeV, or about 4 meters per MeV in air. Note that these values are track-length ranges. Few if any electrons attain these ranges in the direction of the incident beam; typically most will stop far short of these distances.

### 3. IRRADIATION TECHNIQUES

Prior to the use of electron beams, low-energy X-rays were used for total skin irradiation. They presently have limited usage.<sup>73</sup> The clinical results using a variety of such X-rays were less than encouraging because it was difficult to treat the entire skin area adequately. There were maximum field-size and field-junction limitations, and it was not possible to treat to an adequate depth without a large X-ray integral dose.

During this period, a number of TSET techniques, adapted to the equipment available, have been developed. Historically, machine-produced electrons have been used with an accelerator energy range,  $E_e$ , from 1.5 MeV to 10 MeV (prior to scatterers, transmission ion chambers, etc.) for TSET. TSET is now in its fourth decade of use. The Van de Graaff generator, which was the first accelerator employed for TSET, has been largely supplanted by the isocentrically mounted electron linac. Electron beams from accelerators show the typical characteristics of a dose maximum occurring just below a normally incident skin surface and a rapid fall-off of dose with depth to a maximum range determined by the incident electron energy. It is necessary to take suitable precautions in the use of accelerator-produced electrons to achieve a low X-ray background in the treatment procedures and to make certain that the high accelerator beam currents used are properly monitored so that overexposures are not inadvertently administered.<sup>14, 22, 27, 33, 34, 61, 103, 107</sup>

The cumulative dose due to the X-ray component, measured at 10 cm depth and averaged over the patient volume for all fields, typically ranges from 1-4% of the maximum electron dose received at or near the surface. The higher number is associated with higher

energies, non-optimal beam scattering techniques and the use of many fields. A 4% X-ray dose ( $\sim 1.5$  Gy) averaged over the body is considered clinically unsatisfactory by many practitioners.

Studies have been carried out by several centers to determine dose distributions obtained for single-field, multi-field, translation, arc, and patient rotational techniques. Phantom studies suggest that patient rotation, using a rotating platform, provides the best dose uniformity over large portions of the body surface, although the eight-field technique has proved to be almost as good. The six-field technique is simpler to carry out; it provides somewhat less dose uniformity but is considerably better than the two- or four-field techniques.<sup>109</sup> Since the human body is not a simple cylindrical shape, not only are there areas of overexposure, but there are marked underexposed areas which often require supplementary treatments. Patient skin dosimetry measurements are discussed in Section 7.5 and references 27 and 92.

With the use of rotation or multiple large overlapping fields, the typical skin-sparing dose buildup region disappears altogether due to the oblique incidence of many electrons, resulting from the curved patient contours and multiple electron scattering in the intervening air prior to incidence on the patient.<sup>13</sup> See, for example, Figs. 3a, 3b and 3c. The physicist and clinician must take into account the X-ray background as represented by the tail of the depth-dose distribution curve, particularly when high-energy beams are strongly degraded in energy by insertion of a degrader so as to produce a shallower depth dose characteristic of a significantly lower energy beam.

Several linac-implemented treatment techniques incorporate a large, clear Lucite scatterer-energy degrader panel about 1 cm in thickness and 2 m x 1 m in cross section.<sup>25, 43, 71, 94, 101</sup> It is placed about 20 cm in front of the patient and contributes to large-angle scatter of the emergent electrons. This improves dose uniformity, particularly on oblique body surfaces, but reduces penetration and the depth dose falls off at a shallower depth. The panel can also provide a mounting surface for monitor ionization chambers located close to the treatment plane. See Section 5.2 for further discussion on the placement of scatterer-energy degraders.

Brahme has examined the effect of placing a given scatterer near the exit window or at the phantom surface.<sup>16, 53</sup> Although the energy distribution of the two beams is almost identical in such a comparison, the angular distribution of the electrons that reach the phantom are completely different. Electrons reaching the patient from the scatterer placed near the accelerator exit window will have a significantly narrower angular spread than those from the scatterer placed at or near the patient surface. The wider angular spread of the latter distribution results in a higher surface dose and a shallower depth dose due to the decreased practical range because the mean angle of incidence is increased.

### 3.1 Beta particles

Beta particles from radioactive sources, such as strontium-yttrium 90, provide an alternative electron source which because of their wide spatial divergence, broad spectrum of energies and low average energy (1.12 MeV) have a limited penetration depth in tissue (Haybittle, et al.<sup>37-39,47</sup>, Proimos, et al.<sup>95</sup>). Monoenergetic megavoltage electrons have a maximum penetration range of about 0.5 g/cm<sup>2</sup> per MeV in low Z material; their average penetration, as expressed by the depth of the 50% depth dose, is far less. Hence, the penetration depth for beta particles, having a comparable maximum energy, is very much less.

Beta-particle beams from strontium-yttrium 90 have a maximum energy of 2.18 MeV, an average energy of 1.12 MeV, and typical depths cited at the 10% depth-dose level vary from 0.4 to 0.8 g/cm<sup>2</sup>.<sup>47,95</sup> For the largest beta-particle source used to date (24 Ci of <sup>90</sup>Sr + <sup>90</sup>Y), treatment times exceeding 15 minutes are require to deliver 2 Gy by scanning over a patient surface 60 cm x 180 cm.<sup>38</sup> Alternatively, for accelerators, beam-on times of approximately four minutes for doses of one to several grays are typical. In a beta-particle unit described by Haybittle,<sup>38</sup> the 24 Ci source was spread over an area 53 cm long by 2 cm wide. A treatment distance of 40 cm was used, and the source was arranged horizontally with its long axis perpendicular to its direction of motion as it traversed the length of the recumbent patient.

Although beta particles have been successfully employed for TSET, the majority of patients are treated with electrons from accelerators at this time. Long exposure times, lesser average penetration associated with their energy spectrum and poorer uniformity characterize beta-particle treatments. High output and the variable electron energy feature of linacs have led to their increasing adoption for TSET.

### 3.2 Narrow rectangular beams

This section describes techniques used primarily with Van de Graaff accelerators in fixed positions with vertically downward beams, accelerator energies of 1.5 to 4.5 MeV, with patients translated horizontally under such beams. Such techniques are primarily of historical significance and would likely not be a contemporary choice. A translation technique using a linear accelerator has been described by Williams, et al.<sup>116</sup>

In this technique, the accelerator is in a fixed position, and patients are translated on a motor-driven couch placed under the downward-directed beam of electrons.<sup>57,75,76,102,103,111-113,118-120</sup> At the Massachusetts Institute of Technology (MIT-Lahey Clinic Program), the electrons are scattered by Al foils placed near the vacuum window of the accelerator drift tube. They are directed into a conical

collimator having a slit 1 cm x 45 cm wide at its base just above the patient. The slit is perpendicular to the beam axis and oriented at right angles to the direction of motion of the couch. A gaussian distribution of intensity across the width of the cone is obtained with a variation of about  $\pm 10\%$  at a transverse treatment plane 118 cm from the electron window. The patient dose varies as much as  $\pm 15\%$ , as the distance of the skin below the cone changes during treatment. A modified cone design was developed to improve uniformity, reduce the energy loss in the scattering foils, increase the effective dose rate at the patient surface, and reduce the bremsstrahlung background. The shaped slit of this design, wider at the two ends, provides a more uniform dose across the field by having the incident charge uniform over a planar treatment area under the beam. A more uniform dose ( $\pm 3\%$  across the field) was obtained and the variation in dose with patient skin distance from the cone was reduced to  $\pm 8\%$ . The transit time spent under the cone aperture by a point on the skin in the center line of the cone was about one-fourth that of a point 25 cm lateral to each side where the slit was correspondingly wider. One tenth of the accelerator beam current was required for the same dose with the new cone compared to the old.

Patients were initially treated in four positions. Due to the development of some telangiectasia in high dose regions, a six-field and eventually an eight-field technique were developed. Supplementary treatments of obviously shielded or low-dose areas were carried out while shielding regions adequately treated during the multi-field treatments. Internal eye cups were used when eyelids were involved and required treatment; external lead eye shields were used when the eyelids were not involved. In order to minimize the X-ray background, low-Z material was used for shielding of large areas, although small fields were usually shielded by high-Z material such as lead sheet.

Another Van de Graaff TSET technique, once used at the National Institutes of Health (NIH), made use of a wide cone with the beam scanned magnetically in vacuum transversely in the X direction while the patient is moved longitudinally under the beam in the Y direction.<sup>4</sup> The dose distribution across the beam in a treatment plane was uniform to an extent dependent on the distance below the cone but at least as good as  $\pm 5\%$ . The energy of the Van de Graaff accelerator was adjusted to control the depth of penetration for treatment. Treatment times were about one minute for each full length pass and less for small treatment areas.

### 3.3 Scattered single beam

A scattered single electron beam technique employing a linac for a stationary, standing patient has been described by Tetenes and Goodwin.<sup>109</sup> In order to obtain a flattened beam with an electron energy of 4 MeV at the treatment plane, an initial accelerator energy of 6.5 MeV was used with a titanium scattering

foil 0.15 mm thick placed 10 cm from the accelerator exit window. A shaped polystyrene scatterer beam-flattening filter was mounted on the front of the treatment head with a distance of 7 meters between the accelerator beam exit window and the treatment plane. The measured transverse uniformity in the treatment plane for this technique was  $\pm 1\%$  within a 40 cm radius around the central axis and within  $\pm 8\%$  for a 200 cm diameter circle. The maximum dose rate at the treatment plane with both the normal linac scatterer and the added scatterer in place was 3 Gy/min.

Another single-beam technique used to provide large fields makes use of the combined scattering produced by the electron beam window, the intervening air and a specially shaped absorber to flatten the beam.<sup>120</sup> The absorber, thick enough to stop the electrons, is shaped like the hub and spokes of a wheel and placed about 50 cm from the window. At one meter, a 30 cm x 30 cm flat field was produced. The same technique would be applicable to produce a large flattened field with a treatment distance of several meters.

#### 3.4 Pair of parallel beams

In contrast to the long treatment distance of the scattered single electron beam technique described in Section 3.3, Szur et al. describe a technique using two horizontal parallel beams whose axes are contained in a vertical plane at a treatment distance of about 2 meters.<sup>107</sup> The technique was developed for an 8 MeV linear accelerator and includes the use of carbon energy degraders located just beyond the exit window of the accelerator. By using different thicknesses of carbon degraders, the depth of penetration was adjusted from about 2 to 25 mm to meet the requirements of the individual patient. Energy degraders (decelerators) produce less-rapid fall-off of depth dose, as well as a reduction in the beam energy. Two horizontally directed beams, with a central axis vertical separation of 150 cm, were used to obtain  $\pm 5\%$  uniformity for a treatment plane 200 cm high. The X-ray dose was about 2% of the peak value for each field when using a 2 cm thick carbon decelerator. This translates into an average integral dose from electrons of  $75 \times 10^{-5}$  kg Gy per Gy peak dose and that due to X-rays, for a 20 cm body thickness, of  $60 \times 10^{-5}$  kg Gy per Gy peak dose. For thinner decelerators, the integral dose from electrons increased, but that due to X-rays showed little variation.<sup>107</sup>

#### 3.5 Pairs of angled beams

Pairs of angled electron beams, two to eight in number, are the most commonly used method of obtaining large fields for total skin irradiation with isocentrically mounted linear accelerators. This technique is illustrated in Fig. 1 for six pairs of angled beams (six dual fields). An external scatterer is often placed on the front of the treatment head located several meters from the

patient. This geometry results in a reasonably uniform dose distribution at the treatment plane. The two fields overlap, joining at about the 50% level in this plane. The axis of the beam is aimed below the patient's feet for half of the treatment and above the head for the remainder so that the the X-ray fluence of a forward-directed beam. Typically beam angles with the treatment plane 3 meters from the scatterer are  $\pm 20^\circ$ . In one example using 8-MeV electrons at the accelerator window, this treatment technique resulted in an average X-ray background of about 0.7% for each dual field. This TSET treatment technique is described in detail in Section 4 for the case of six pairs of angled beams (dual fields). The dosimetric features of such multiple field beams are described in Sections 6.4 and 7.5. Some clinical findings have been reported by Bagshaw, Hoppe, et al.<sup>7, 44, 45</sup>

### 3.6 Pendulum-arc

A technique described by Sewchand et al.,<sup>101</sup> uses an isocentrically mounted 8 MeV linac. The accelerator is rotated continuously during treatment in a  $50^\circ$  arc about the isocenter starting from an initial angle with the beam axis aimed below the feet to a final angle with the beam aimed above the head of the standing patient. It may be feasible to vary the dose rate, or gantry rotation speed at constant dose rate, automatically, as a function of gantry angle so as to vary the dose rate and hence, optimize the dose uniformity in the vertical direction. A large Plexiglas sheet 1 cm thick placed 5 cm from the patient is used to degrade the beam energy further and provide large-angle electron scattering near the patient skin as described earlier. A six-arc-field technique is described with the total X-ray dose measured at 10 cm depth equal to 4.2% of the average electron dose at  $D_{\text{max}}$ .

### 3.7 Patient rotation

Studies of treatments involving patient rotation about a vertical axis for total skin irradiation include the work of Tetenes and Goodwin<sup>109</sup>, Podgorsak et al.<sup>94</sup> and Kumar.<sup>71</sup> These groups use a single horizontal beam, the first with a single scatterer located near the beam exit window and a 7-meter treatment distance. The latter two groups have a first scatterer placed near the beam exit window and a second large planar scatterer located 20 cm from the treatment plane, which is located 265 cm and 3 m, respectively,<sup>71,94</sup> from the beam exit window. Podgorsak et al. have developed analytical expressions for rotational dose distributions using stationary depth-dose data and a variety of phantom and patient cross sections.<sup>94</sup> The calculated and measured dose distributions show close agreement.<sup>91</sup> With an accelerator electron energy of 6 MeV and a depth-dose curve equivalent to 3.5 MeV in the treatment plane, the X-ray background amounted to 4% compared to 2.2% for the Tetenes and Goodwin

method.<sup>109</sup> Rotation therapy can reduce setup and treatment times and simplify beam matching as well as compensate for some patient motions, but problems arising from self-shielding by limbs are not significantly ameliorated. Kepka and Johnson have combined the dual-field technique with patient rotation to improve dose uniformity.<sup>63</sup>

#### 4. SIX-DUAL-FIELD IRRADIATION TECHNIQUE

The six-dual-field technique involving six patient orientations is described in detail so as to provide the reader with an overall perspective of one widely used treatment method. However, this emphasis is not intended to prejudice the adoption of other TSET treatment techniques which may be more suitable for particular accelerators and environments. The treatment technique described and illustrated herein pertains primarily to the later development of the six-dual-field technique.<sup>91</sup> With the exception of Figs. 3c and 4, the accompanying figures are for the technique currently used at Stanford. The technique was modified in 1973 to provide a higher energy than used originally.<sup>59</sup>

##### 4.1 Irradiation geometry

The six-dual-field technique widely used with isocentrically mounted linacs employs pairs of angled beams as shown in Fig. 1a, with the patient standing in six angular orientations about a vertical axis, three each an alternating days as shown schematically in Fig. 1b. Four of the six patient orientations are illustrated in Fig. 1c, the remaining two obliques are not shown. This particular combination of six dual fields provides acceptable dose uniformity and low X-ray dose to the patient. Although moderately complex, it may be implemented on many contemporary isocentric linacs in moderately sized treatment rooms.

##### 4.2 Beam characteristics at treatment plane

Dosimetric characteristics of TSET beams are examined for a single horizontal beam, a single angled dual-field beam, and the full array of six dual-field beams. These parameters include depth dose, isodose distributions, field flatness in the treatment plane and X-ray background.

###### 4.2.1 Single horizontal beam

The characteristics of angled dual fields can be more easily understood by first examining the features of a single horizontal beam in the treatment plane. Fig. 3a shows the relative central axis, depth-ionization curve for such a beam at the calibration point of Fig. 1a, a treatment plane midpoint approximately 3 m distant from a scatterer placed on the front of the treatment head. The curve portrays relative ionization vs. depth in g/cm<sup>2</sup> of polystyrene. The depth-ionization curve is expected to differ

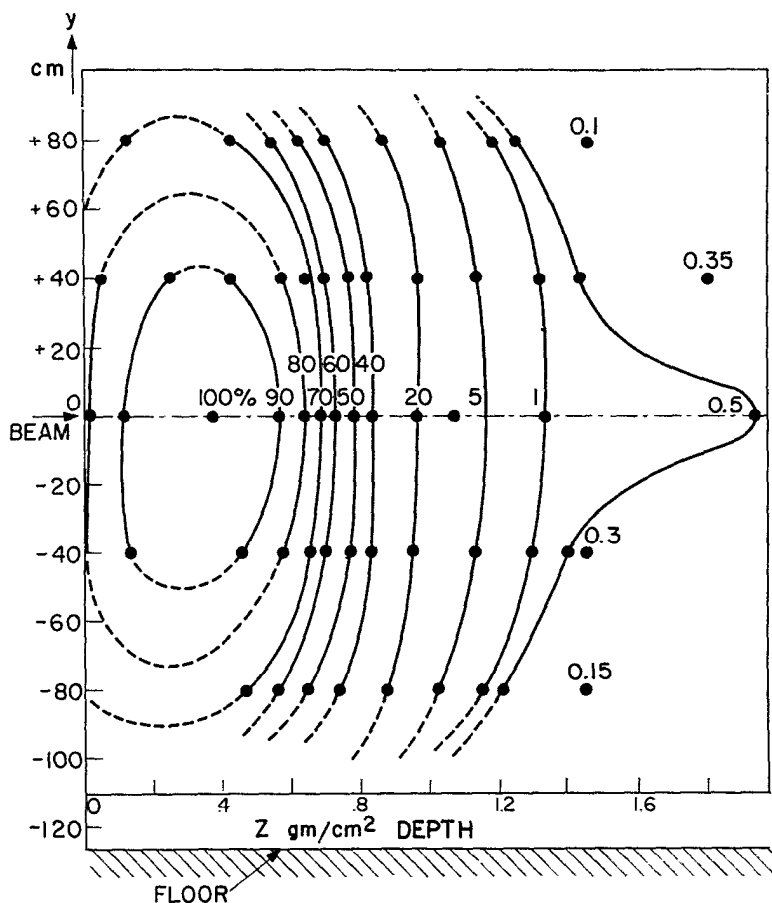


Fig. 4. Isodose distribution in the  $y$ - $z$  plane for  $x = 0$  and  $\theta = 0$ . This distribution is constructed from depth-dose curves similar to Fig. 3b, but taken at various points in the treatment plane and at a lower incident electron energy. Dashed portions of the curves are extrapolations (Karzmark et al.<sup>59</sup>).



insignificantly from the depth-dose curve for electrons below 10 MeV.<sup>84</sup> The scatterer consists of 1 mm Al plus 12 mm (1.2 g/cm<sup>2</sup>) of Presdwood. The Presdwood was added as a degrader to limit the beam penetration to that desired by the clinicians. The dose, 93% at the surface, reaches maximum near 0.3 g/cm<sup>2</sup> depth and falls to near zero at 2.4 g/cm<sup>2</sup> depth as illustrated in Fig. 3a. The X-ray background is seen to be 2% on this central axis curve. Using the range-energy relationship of Section 2.1, the practical range of 1.98 g/cm<sup>2</sup> polystyrene (equivalent to 1.92 cm of water) yields an electron energy of 4.2 MeV at the treatment plane for an accelerator electron energy of about 8 MeV. The energy and penetration will be less for a pair of dual-angled beams because of their obliquity to the treatment plane. In addition, the average penetration depth below the skin surface of a patient placed in all six angular treatment orientations will be significantly less than the depth of maximum dose for a normally incident beam, particularly for angled beams incident on inclined body surfaces (see Figs. 3b and 3c). Because of energy losses in the intervening air (at least 0.25 MeV/m), and especially in the scatterer and degrader, energy losses totaling about 3.8 MeV occur between the exit window of the accelerator and the treatment plane in this particular example.

Figure 4 illustrates the isodose distribution in a vertical plane through the central axis at 3 m distance for a beam similar to that in Fig. 3a, but about 1 MeV lower in energy and with a lower X-ray background.<sup>59</sup> Note that the X-ray background of 0.5% is strongly peaked in the forward direction and falls rapidly for off-axis points. It is clear that such single fields do not adequately cover the patient's body height, so that much longer distances or multiple beams must be used. The use of the narrow pencil beams in designing treatment beams for TSET has been explored.<sup>41a, 74</sup>

#### 4.2.2 Dual-field beams

Two angled fields can provide improved dose uniformity over areas the size of patient dimensions. In this technique, two equal exposures are given, one from each of the two angled components of a dual field as shown in Fig. 1a. Fig. 3b illustrates a typical relative depth-dose curve in water for a single dual field and for six dual fields at  $\theta = \pm 20^\circ$  for the same linac operating conditions as for Fig. 3a. The most probable electron energy,  $E_{p,0}$ , at the phantom surface for the single dual field is 3.8 MeV as calculated from the practical range  $R_p$  of 1.7 cm using the range-energy equation. The mean electron energy,  $\bar{E}_e$ , at the phantom surface for the single dual field, is 2.6 MeV as calculated from the  $R_{50}$  range of 1.1 cm. The forward-directed X-ray peaks from such dual fields are directed above and below the standing patient, resulting in the X-ray background profile given in Fig. 5; its average is about 0.7% for a single dual field and about 1.5% for the full six-dual-field irradiation (at any point, three dual

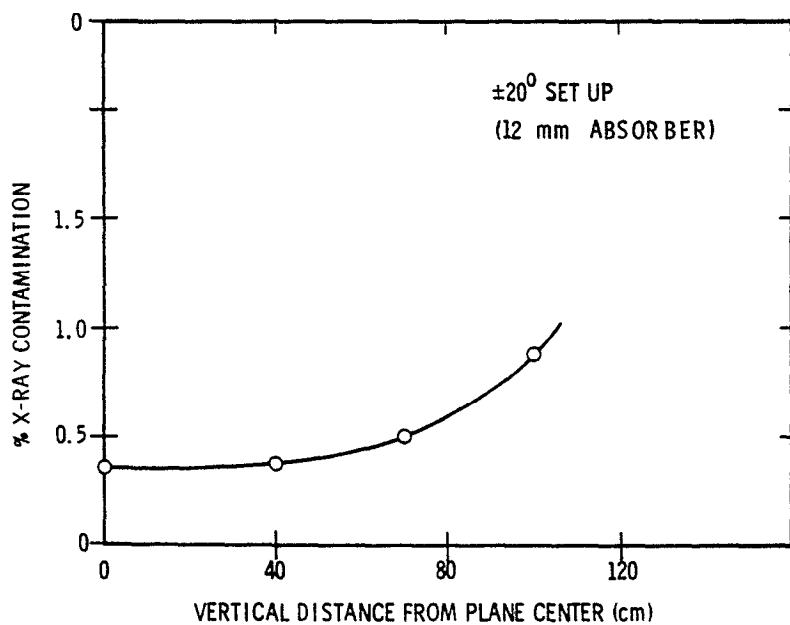


Fig. 5. Relative X-ray background in the y direction at  $x = 0$  for a single symmetrical dual-field. Measurements were made at a depth of about  $4.0 \text{ g/cm}^2$  of polystyrene.

fields contribute to electron dose and six to X-ray dose).<sup>59</sup> The X-ray background may vary from one accelerator to another for the same beam energy and depends significantly on the scatterer-degrader materials in the beam. A composite dose distribution at the depth of dose maximum, 0.34 cm, is shown in Fig. 6.<sup>59</sup> Uniformity is within  $\pm 4\%$  over substantially all of the body area in this plane. The angle  $\theta$  between the horizontal and the beam central axis, as shown in Fig. 1a, is chosen to provide the best dose uniformity along the vertical direction at the depth of dose maximum as shown in Fig. 6. The optimum angle and associated gap between the light field edges will depend on beam energy and scattering conditions. A vertical array of small films exposed to a single dual field can be used in choosing this angle.<sup>64</sup>

#### 4.2.3 Six dual-field beams

When the patient is placed in all six positions, with a dual-field irradiation at each position, the depth dose is considerably less uniform than indicated in Fig. 6 due to body curvature, the varied angles of electron incidence and the finite number of beam orientations. The six patient orientations are spaced at 60-degree intervals, resulting in a variation of dose that has a 60-degree periodicity. As seen in Fig. 7, this variation is approximately  $\pm 10\%$  at the surface, dropping to  $\pm 5\%$  at a depth of 3 mm. The most dramatic effect, however, is the very rapid fall-off of dose with depth for the full six dual-field irradiations. This has been documented by film and TLD dosimetry. Limited film results are shown as the triangular data points in Fig. 3b. Fig. 3c from Fraass<sup>27</sup> compares 4 MeV depth doses for a single field using a horizontal beam in water with all 12 fields (six dual-fields) using film in a humanoid phantom. The 12-field data of Fig. 3c and the triangular data points of Fig. 3b are mean depth dose. They were obtained by averaging the dose at the depth of dose maximum from a circular traverse around a 30 cm cylindrical phantom located at the treatment plane midpoint.

### 5. LINAC OPERATING CONDITIONS

#### 5.1 Linac operating parameters

These operating parameters include linac beam current and energy together with collimator settings and possible machine modifications. Stable, repeatable linac operating beam energy is central to satisfactory TSET therapy. Energy changes can shift the long SSD-distance fields laterally and markedly change dose calibration and uniformity in some linacs. A high average linac beam current is needed to provide an adequately high dose rate in the patient treatment plane several meters distant (e.g., at least 0.25 Gy/min at  $D_{max}$ , the dose maximum). Dose rates at the patient of 1 Gy/min or higher are desirable in order to reduce treatment times and thus minimize patient motion and fatigue. The

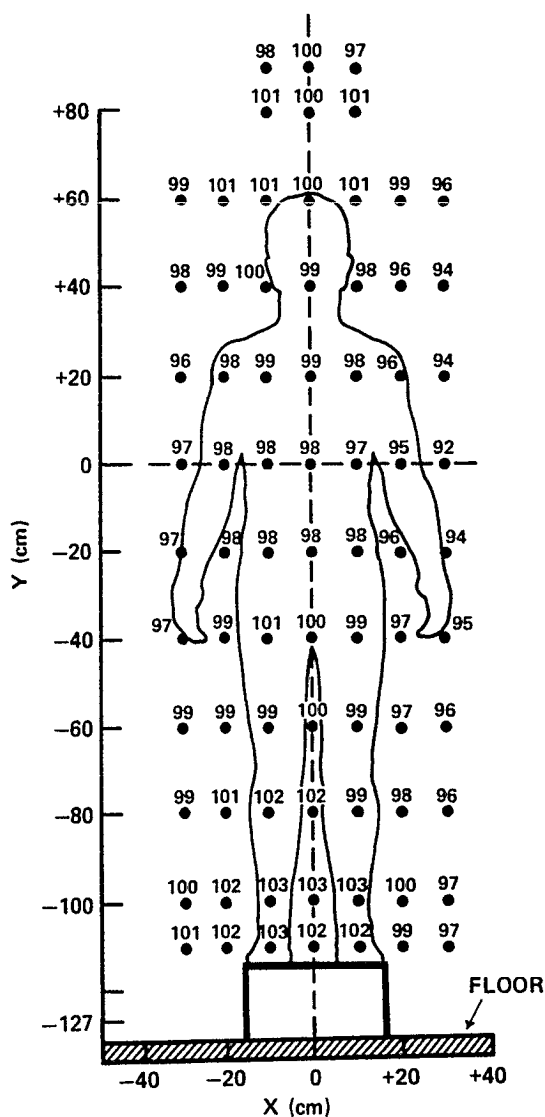


Fig. 6. Composite isodose distribution in the x-y plane for  $z = 0.34$  g/cm polystyrene. The two component beams were angled at  $\pm 20^\circ$  and normalized to 100 at the points ( $x = 0$ ,  $y = \pm 60$  cm).

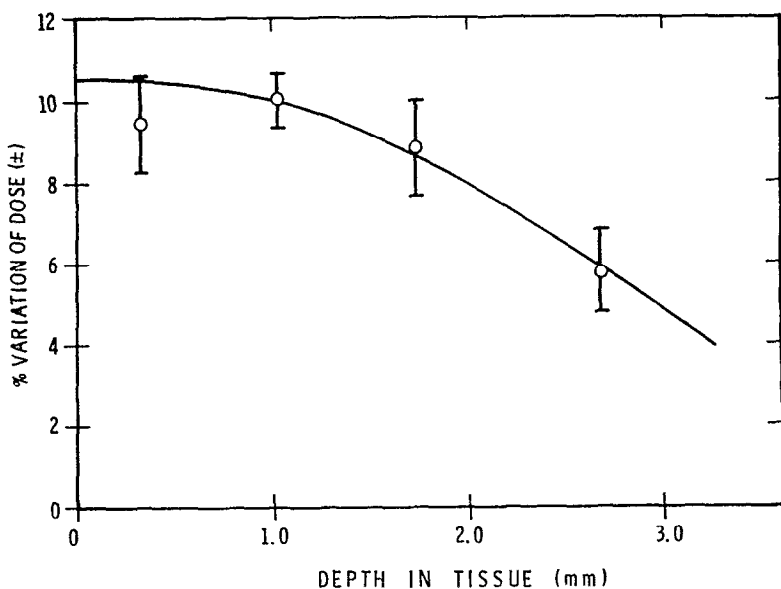


Fig. 7. Percentage dose variation vs. depth in a 30 cm diameter circular phantom. Obtained for six dual-fields from a circular traverse around the phantom exposed at the level of the calibration point (see Fig. 1a). A smooth curve has been drawn through data points whose variation around the phantom is illustrated by the vertical spread between the bars.

average beam current is directly proportional to the modulator pulse repetition frequency times the pulse length, i.e., the duty factor or fractional beam-on time, a pure numeric, which is typically about 0.001. Hence, for such a duty factor, peak beam currents during the pulse are a thousand times larger than their average values and peak currents expressed in milliamperes convert directly to average currents in microamperes. Average beam currents for conventional therapy linacs operating in the X-ray mode range from about 20 to 200 microamperes corresponding to electron beam energies of 25 to 4 MeV, respectively. Typically, X-ray production varies as the cube of the incident electron energy in this energy range. At high X-ray energies, the flattening filter absorbs a significant fraction of the central axis beam intensity; as much as 90% at 25 MeV. A representative 6 MeV linac in the X-ray mode operates with 50 microamperes average beam current. Some manufacturers can provide machines with substantially higher beam current capability on special order. Because of the large inverse square law dependence and scattering losses, the low-energy electron mode for TSET typically requires an average beam current comparable in magnitude to that for 4 to 6 MV X-ray production. For some techniques, the beam current may be 100 or more times greater than required for conventional electron therapy of comparable energy at 100 cm SSD. The X-ray collimator jaws are usually opened to the largest field size and may be rotated 45° with respect to the vertical for TSET. The long diagonal of the field which results, improves needed vertical dose uniformity. It also increases output slightly due to in-scatter from surrounding air and, thus, reduces the required beam current.

Edelstein, et al.<sup>25</sup> have observed that detuning their 6 MeV linac to reduce beam energy resulted in a 0.25 MeV energy change and a 3 mm shift in electron depth dose. However, there was a significant accompanying change in beam symmetry associated with their nominal 90° beam bending system. This change would be apt to be less significant in a nominal 270° achromatic beam bending system. The addition of polystyrene absorbers was found to be a more satisfactory means of reducing the energy than detuning.

It is recommended that linac operating conditions related to dosimetric and safety aspects be determined by experiment after consultation with the manufacturer and users of similar units for TSET. Once a TSET technique has been experimentally investigated and performance demonstrated, it is desirable to establish and adhere to a written procedure protocol for carrying out TSET, including the changeover to and from this modality. A test run after changing modality to observe accelerator operation and dose monitoring is an essential aspect of the procedure. See Table I for an example procedure.

## 5.2 Beam scatterer-energy degraders

The provision of large, uniform, low-energy electron fields

for TSET entails the interposition of materials to scatter the beam and may require additional material to reduce the beam energy to a desired value from an available higher energy. Thick materials used primarily for this latter purpose are termed "energy degraders" or "decelerators." Thin materials used primarily to spread out the beam are termed "scatterers." Interposed material both scatters the incident electron beam and reduces its energy as well as generating a contaminant megavoltage X-ray background. All three processes occur in a given material, but their proportions are different functions of the atomic number,  $Z$ , of the material, and of beam energy. The selection and placement of scatterers and degraders are strongly influenced by the need to minimize the background radiation. It should be kept in mind that scatterers also act as degraders, and vice versa, even when a material of appropriate  $Z$  is selected. Beam scatterer-degraders are placed internally in the treatment head or externally, either on its front surface or at a location between it and the patient. The position along the beam axis of the material used to degrade the beam energy is important in determining the electron dose rate, uniformity, depth dose and relative X-ray background over the treatment plane because of its effect on electron scattering. Placement of large scatterer-degraders near the patient is described in Sections 3.0 and 5.2.

If the scatterer is located adjacent to the accelerator electron window, the collimator aperture might, in some linacs, unduly restrict electron field size and uniformity for TSET, and the accompanying X-ray background would likely be high for a given electron dose and uniformity. This follows since a higher beam current with a proportionally higher, accompanying X-ray background is needed for a given dose rate in the treatment plane. Large-field flatness is improved significantly by scattering of electrons from the several meters of air between the treatment unit and the treatment plane, especially by electrons scattered back into the treatment field from air outside the volume enclosed by straight lines from the source to the rectangular patient plane. Hence, the 2 steradian scattering solid angle for scattering materials placed at the front of the treatment head should not be restricted by an aperture.

Additional scatterer-degraders may be placed at the front surface of the treatment head. If improving uniformity is the criterion, a high- $Z$  material is desirable since it maximizes scatter per unit of energy loss. Scattering and X-ray production exhibit a similar dependence on  $Z$ . Placing the scatterer-degrader on the treatment head front surface, usually about 50 cm from the accelerator beam exit window, concentrates X-ray production along the beam central axis and X-ray intensity is high relative to electrons in the treatment plane. Kumar, et al. find that for a 6 MeV accelerator electron beam, a relative X-ray intensity of  $> 15\%$  results when a 9.6 mm Plexiglass scatterer-degrader is mounted on the collimator front surface.<sup>69</sup> When mounted as a large panel 15

cm from the patient, the X-ray intensity is reduced to  $< 2\%$ . However, as noted above, the particular dependence of scattering and X-ray background on atomic number  $Z$  and electron energy may render this reduction in X-ray background, in part, illusory when electron dose uniformity, depth dose and integral X-ray dose are assessed.

All scatterers should be interlocked because their removal could give rise to a significant radiation hazard. The accelerator electron window, and internal ionization chamber if left in place at its normal location, function as partial scatterers, but ion recombination in the high-intensity beam may preclude the latter's use for monitoring.<sup>52</sup> As a consequence, an external monitor chamber is often placed further from the accelerator window at the front surface of the treatment head or in or near the treatment plane located some meters distant.

If the accelerator operates more stably at a higher energy than desired for treatment, additional degrader is needed to retain stable operation with adequate dose rate and flatness. For a given energy reduction in this case, the use of a low- $Z$  material will minimize X-ray production as well as scattering. By placing the degrader near the accelerator electron exit-window, the beam is scattered leading to reduced electron intensity at the internal ionization chamber or at the treatment head front surface where the scatterer and monitor ionization chamber may be located. This reduced intensity improves ion chamber saturation and simplifies beam monitoring.

### 5.3 Beam monitoring

The subject of electron beam monitoring has been reviewed in ICRU Report 21<sup>51</sup> and briefly in its successor, ICRU Report 35.<sup>53</sup> The parameter monitored is usually the electron fluence rate or indirectly, the absorbed dose rate at  $D_{\max}$  or the absorbed dose at some point deeper in the irradiated object. However, other parameters may also be monitored such as beam symmetry, uniformity, electron energy, or relative depth dose. The response of the monitor, including associated electronic processing devices, should, as far as possible, be directly proportional to the parameter of interest, and the constant of proportionality should be independent of other parameters of the beam. Monitors must be calibrated, and their calibration should remain constant over extended periods of time. Monitors for TSET may include the built-in internal transmission monitors located in the treatment head or external monitors located either on its front surface or at or near the patient treatment plane.

Full-field monitoring devices include transmission ionization chambers, secondary electron emission monitors, and electromagnetic induction monitors.<sup>51</sup> These devices are placed where the electron beam emerges from the accelerator and have the advantage



of leaving the useful beam free for apparatus or patients. Partial-beam monitoring (sampling) devices include ionization chambers, collector monitors, and Faraday cups. They have the advantage of being able to monitor that part of the beam which is close to the patient instead of the total beam as it emerges from the accelerator. TSET monitors are usually ionization chambers or electron collectors. The usefulness of beam monitors placed in or near the treatment head depends markedly on the stability of accelerator operating conditions. Stable monitoring of patient treatment-plane dose requires stable electron-beam energy and accurate reproduction of radiation-field geometry between monitor and patient as well as the absence of obstructing material inadvertently placed between monitor and patient, conditions sometimes not maintained in practice. In particular, the dependence of the mean electron scattering angle on the inverse of the square of the energy, renders the system vulnerable to energy variations of the beam. Additionally, nonachromatic magnets (e.g., nominal 90°) are prone to move the radiation field laterally by significant amounts for changes in beam energy, and can seriously alter beam uniformity and calibration.<sup>25</sup> A frequently used combination for TSET monitoring involves a full-beam transmission ionization chamber at or within the treatment head and a sampling chamber or electron collector placed at or near the patient treatment plane but not in line with the patient. Activation of a sampling monitor can be incorporated in the interlock chain for TSET and give notice of the absence of an electron applicator. Many centers employ a backup timer to limit the maximum treatment time.

Ionization chambers have high sensitivity but may have significant ion recombination. The high fluence rates of pulsed linac beams can reduce their ion collection efficiency, accuracy and usefulness. Hence, the collection efficiency of the dose-monitor ion chamber for TSET needs to be assessed. It is recommended that a conventional ion chamber saturation curve (collected charge vs. inverse voltage) be obtained to establish whether or not the ion chamber current is represented by the Boag theory. If it can be, then a simple two-voltage technique for accessing collection efficiency in pulsed beams can be used thereafter.<sup>52</sup> Several radiotherapy linacs now incorporate magnetically swept electron treatment beams. Conere and Boag have extended the two-voltage assessment techniques to such beams.<sup>21</sup>

Electron collectors, which include Faraday cups and collector monitors, sample fluence rather than absorbed dose. However, since the stopping power of tissue (excluding radiative stopping powers) is a very slowly varying function of energy above 500 keV, the absorbed dose per unit fluence is nearly constant for small changes in beam energy.<sup>51, 84</sup> Although the sensitivity of collector monitors is low and may preclude their use in the treatment plane at low dose rates, their freedom from saturation problems has led to their use by several centers.<sup>1, 11, 52, 118</sup> Like the Faraday

cup, they absorb and collect the incident electron fluence over a defined area. The Faraday cup is evacuated but electron collectors operate at atmospheric pressure. Their absorber is electrically insulated and shielded from the outside air so that air ions from the surroundings are not collected. The Faraday cup, which is often used as an energy independent detector, has been reviewed in ICRU Report 21 and elsewhere.<sup>51, 59</sup>

All beam monitoring systems require that dose at some relevant site or plane be unambiguously and repeatably related to a Monitor Unit (MU) value read out at the control console. Conventional electron and X-ray monitoring systems for normal treatment distances, typically 100 cm, incorporate a dual-channel redundant system. Usually, two or more full-field transmission ionization chambers are located within the treatment head. Their outputs are connected to electrometer amplifiers to provide two independent indications of integrated dose and one of dose rate. A calibration stability of  $\pm 1\%$  is attainable for conventional treatment modalities.

Beam monitoring for TSET is significantly more complex and uncertain than for conventional X-ray and electron modalities. Redundancy is essential in order to protect the TSET patient from the overexposure due to failure of one integrating dose monitor. The two monitors must be completely independent so as to preclude any common mode failure which could lead to excessive dose being delivered. Such factors as the large linac beam current, fluctuations in beam energy, the large SSD values, the interposition of one or more discrete scatterers, the effect of air scattering, and variation in patient or machine positioning combine to introduce large variations in calibration stability and justify appropriate operational precautions.

There are three choices in the location of the monitoring ionization chamber:

- (a) Existing transmission chamber(s) in the treatment head located about 25 cm or less from the accelerator vacuum window.
- (b) External chambers placed at or near the front surface of the treatment head about 50 cm from the electron source.
- (c) External chambers located at or near the patient treatment plane, usually 2 to 7 meters distant.

Typically, between the patient treatment plane and the internal linac ion chamber, an inverse square dose reduction of the order of 100 or more combines with a reduction due to scattering of 10 to 100, yielding an overall dose reduction that may be significantly greater than  $10^3$ . This large factor gives added significance to the recommendation that beam monitors be placed distal to beam-modifying components since the latter's omission or removal can drastically increase patient dose. It is desirable to monitor the radiation field at the treatment plane and to integrate the

output of such distant monitors directly into the control-console dose read-out system. Alternatively, the distant monitor can be used to correlate partial-beam, treatment-plane monitoring with the response of an ion chamber located in the treatment head or at its front surface. At least one manufacturer provides facilities to terminate the irradiation with an external dosimeter instead of the built-in dose measuring system.

The six-dual-field TSET technique described in detail in Section 4 provides a dose rate of 0.25 Gy/min (0.60 Gy/min for the straight-ahead beam) at the treatment plane 3 m from the ion chamber-scatterer located on the front of the treatment head.<sup>91,92</sup> The dose rate at the front of the treatment head, 50 cm from the electron source, is about 180 Gy/min for Stanford's particular ion chamber with a collection efficiency of approximately 80%. The ratio of these dose rates, 300, decreases with increasing energy.

## 6. DOSIMETRY AND INSTRUMENTATION

Dosimetry for TSET is difficult and complex because of the need to measure and evaluate absorbed dose at shallow depths over a large area in the patient treatment plane. Such large spatial fields do not lend themselves readily to measurement with conventional linear scanners and isodose plotting equipment. The short ranges of the electrons necessitate special attention if the dosimetry and calibration of such beams are to be accurate. Many radiation detectors are too thick for these high-gradient depth-dose fields, or exhibit significant variations in directional response. The electric currents generated by small-volume, high-resolution ionization chambers are often so small that noise and spurious signals arising from irradiation of the signal cable become dominant. However, by selecting suitable detectors and instrumentation, observing appropriate precautions and exercising care, valid dosimetry data for use in patient treatment can be obtained.

### 6.1 Dosimetry methods

There are many radiation detectors available for general data acquisition, but choosing the right one for TSET is important. The detectors suitable for this task include ionization chambers, film, thermoluminescent materials, Fricke dosimeters, electron collectors, and Faraday cups. It is imperative to know in detail how each functions so that advantage can be taken of the special features of each.

For scanning in a water phantom, small thimble ion chambers, with well-studied polarity and saturation effects, are needed. They should have air volumes with linear dimensions of a few millimeters or less. Small-volume, parallel-plate ionization chambers having a thin window and shallow active depth (about 1 mm)

are advantageous for depth-dose data acquisition in a flat solid phantom. Depending on its design, the ion chamber may exhibit polarity effects. In addition, the ion chamber cable, if irradiated, may exhibit extreme polarity effects, but these can be reduced by shielding it from electrons. It is necessary that the response for the two collecting-voltage polarities be averaged for each dose (ionization) measurement.

Semiconductor diode detectors, if proven reliable when compared directly with small ion chambers in similar electron beams, can be useful for measurements with good spatial resolution.<sup>36</sup> Film can provide data rapidly over large areas, but is subject to error.<sup>77</sup> Film may be used with plastic or water phantoms. Film dosimetry is reviewed in a number of publications.<sup>3, 8, 41, 77</sup> Energy dependences of the detector, which can be significant, particularly for film, must be investigated and if necessary, used to correct data. If film is used, care should be taken to eliminate even the smallest air gaps when electrons traverse it at or near grazing incidence.<sup>77</sup> The film density vs. dose response to electron irradiation needs assessment in the energy range involved. Several film techniques particularly useful for TSET dosimetry have been described by Bagne and Tulloh.<sup>6</sup> TLD chips, cubes, and wafers are valuable, but their accuracy must be confirmed against ion chamber data, and their anisotropy for low energy electrons must be studied. TLD powder in capsules or packets is sometimes too bulky to provide adequate spatial resolution. Small TLD dosimeters, ideally thin layers of powder confined between tape or 1 mm cubes taped to the skin, can be very useful for *in vivo* dosimetry to assess the uniformity of dose and confirm monitor calibration.<sup>27, 92</sup> Ion chambers or diodes, taped to the patient, are not as practical, except for occasional single-point measurements.

Much of the data can be taken with any of the detectors mentioned earlier, but the absorbed dose calibration must be done with an NBS-traceable ion chamber. In order to reduce possible complications and errors that may come about when attempting to calibrate low-energy electron beams, the chamber used must satisfy appropriate criteria relating to materials employed, geometrical construction, and saturation properties.<sup>1, 42, 43, 50</sup>

## 6.2 Dosimetry phantoms

Since no solid material mimics tissue precisely with respect to energy loss and scatter, water-phantom depth-dose data are usually obtained as a reference. Polystyrene, which has an electron density very close to that of tissue, is the most suitable material for a solid phantom. The magnitude of the charge storage problem in electron irradiated plastic phantoms is becoming resolved at the time of writing.<sup>30, 40a, 110</sup> Hence, the reader is advised to keep abreast of developments in phantoms for electron beams. Conducting plastics or thin laminae of polystyrene (or

Mylar) with (or without) conductive graphite coatings are recommended. Layered, flat phantoms are employed for obtaining depth-dose and buildup data, but elliptical, oval or cylindrical phantoms of appropriate radii are useful for simulating patient body and limb cross sections.

### 6.3 Dosimetry measurements

A wide variety of dosimetric measurements are carried out in developing a TSET technique. They are described in this section and usually include electron energy, fluence, depth dose, isodose and X-ray contamination measurements. Absorbed dose measurements are treated separately in Section 6.5. As the beam passes through the exit window and before reaching the patient treatment plane, the electron beam is scattered and further spread out and degraded in energy by passing through a sequence of materials consisting of the exit window, scattering foils, monitor chambers, perhaps the field illumination mirror, intervening air, and additional degraders (used mainly to reduce the beam energy and penetration). For TSET, the average energy loss occurring in this sequence is typically 1 to 2 MeV but may be higher if thick energy degraders are employed.

At the phantom surface, the mean energy of TSET beams,  $\overline{E}_e$ , may be significantly less than the most probable energy,  $E_{p,e}$ , as seen from the following example for the depth vs. ionization curve of Fig. 3a. The most probable energy,  $E_{p,e}$  in MeV, can be calculated by the range-energy equation given in Section 2.1. Depth absorbed dose and depth ionization curves in a water phantom give the same value of  $R_p$  within about 1 to 2 mm.<sup>84</sup> Using this equation for Fig. 3a yields an electron energy of 4.2 MeV at a practical range  $R_p$  of 1.92 cm of water at the treatment plane for an accelerator energy,  $E_a$ , of about 8 MeV. The mean energy at the treatment plane for the half-value depth  $R_{50} = 1.33$  cm in Fig. 3a yields a mean energy of about 3.1 MeV, a value significantly less than the most probable energy value of 4.2 MeV for this single horizontal beam.

A number of factors combine to make uncertain how best to evaluate absorbed dose for TSET electron beams. Wide variations of dose to different areas of the body result from the geometric complexities of beam and body angulation. The absorbed dose for electrons is a function of the stopping-power ratio. For the range of mean energies  $\overline{E}_e$  of TSET electrons, the stopping-power values vary by approximately 10 per cent.<sup>84</sup> The wide energy range and incident angular spread of TSET electrons create additional uncertainty in absorbed-dose evaluation.

It is recommended that the most probable energy,  $E_{p,e}$ , as determined by the Markus equation for a single horizontal beam at the treatment plane, be employed for energy specification of an electron beam for TSET. In addition, it is recommended that the

mean electron energy,  $\bar{E}_0$ , determined by the half-value depth  $R_{50}$ , for a single dual-field, be employed for dosimetry of energy-dependent calibration factors in calculating absorbed dose at the calibration point as described in Section 6.5. Both  $E_{p,0}$  and  $\bar{E}_0$  refer to values at the phantom surface, see Fig. 2.

A simple but relevant measurement of incident electron fluence can be carried out with an evacuated Faraday cup.<sup>51,59</sup> A collimator of known area is placed over the aperture of the cup and the electron fluence determined from the collected charge and the area of the collimator. An estimate of the entrance surface dose can be obtained from this fluence measurement at the treatment plane, the mean electron energy, and an appropriate collision mass stopping power. It is reassuring to have such estimates to confirm ionometric findings when working with low-energy electrons. The electron charge fluence incident on the skin for a dose of 1.0 Gy corresponds to about  $0.50 \text{ nC/cm}^2$ .<sup>112</sup>

Depth dose data can be acquired with a parallel-plate ionization chamber overlaid with varying thicknesses of polystyrene absorber. A small amount of polystyrene surrounding the chamber suffices for this measurement. It has been found useful to erect a plywood panel with a coordinate grid just behind the patient treatment (x-y) plane and to provide a method of positioning the chamber plus absorbers at defined points in the treatment plane using the coordinates of the grid (Fig. 1a). The assessment of radiation field uniformity and construction of isodose patterns at relevant depths, z, beyond the treatment plane, can be achieved by combining depth-dose data from an appropriate selection of points in the (x,y) field for each absorber thickness.

Dosimetry data can often be acquired rapidly by employing ion chambers or diode detectors with a linear scanner in air or with an x-y-z isodose plotter in a water phantom. Often, these spatially restricted field measurement data may be combined by moving the equipment so as to overcome the lateral scan limitations.

In-phantom dose distributions for the different irradiation techniques for various body sections constitute important data, but unfortunately are difficult to obtain due to the curved surfaces of the body and the low energy of the beam. Film and TLD, due to their good spatial resolution, are recommended for these assessments but require careful procedures to ensure accuracy.

Some insight into the complex phenomena involved in low energy TSET beams has been provided by the theoretical studies of Berger, Brahme, Hubbell, Seltzer and others.<sup>10,11,16,100</sup> The idealized, narrow-pencil electron beams, which constitute the starting point of such studies, are monoenergetic and normally incident on a semi-infinite water phantom at  $z = 0$ . Broad-beam, absorbed-dose distributions are constructed by the superposition of these elementary beams. The penetration of such broad beams is

significantly greater than for the narrow pencil beam: their peaks lie higher and at a significantly greater depth. Calculations using the Monte Carlo method are simplified by use of the Continuous-Slowing-Down Approximation (CSDA). The CSDA exists in theory only. It involves a rectified path length which ignores the angular deflections of scattering and considers only collision energy losses. The CSDA range,  $r_0$ , is the mean path length for an electron of kinetic energy,  $T_0$ , and is derived by integrating the reciprocal of the total stopping power over the energy range extending from  $T_0$  to zero. Seltzer, et al.,<sup>100</sup> then proceed to incorporate the modifying effects of energy loss straggling, multiple scattering angular deflections and the production and transport of both bremsstrahlung photons and knock-on electrons. This publication<sup>100</sup> contains many informative illustrations including normalized broad-beam depth dose curves which incorporate the modifying effects noted on the simple CSDA straight-ahead approximation. They find that the practical range of such curves,  $r_p$ , defined like  $R_p$  earlier, varies in terms of  $r_0$  as follows: The ratio  $r_p/r_0$  varies from about 0.93 to 0.97 over the range of  $T_0$  from 3 to 7 MeV, respectively reaching 1.0 at about 10 MeV. The ratio  $r_0/T_0$  is constant to within several percent over this energy range. The practical range,  $r_p$ , for their constructed, broad-beam, theoretical depth-dose distributions is given by:

$$r_p = 0.505 T_0 - 0.106$$

which specifies a somewhat deeper penetration than the Markus equation for measured clinical depth-doses as given in Section 2.2.1. Here,  $r_p$  is the practical range in cm of water and  $T_0$  the kinetic energy in MeV of the normally incident electron beam.

The half-value depth in water,  $z_{50}$ , at which the dose of the constructed broad beam curve has fallen to 50% of its peak value, lies somewhat deeper than the clinical  $R_{50}$  depth defined earlier. Such theoretical incident beams are "cleaner"; their relative surface dose is lower and their dose maxima lie deeper than for the clinical beams used in therapy. We can define a coefficient  $k'$  for these theoretical beams by the equation  $T_0 = k' z_{50}$  which is analogous to the constant  $k$  in the equation  $E_0 = k R_{50}$  and where  $R_{50}$  is the half-value depth in cm of water and  $E_0$  represents the mean electron energy arriving at the phantom surface, see Fig. 2. Using data of Berger and Seltzer, the value of  $k'$  is found to vary slowly from 2.57 to 2.38 over the range 3 to 7 MeV, respectively, and falls to 2.33 at 10 MeV, the recommended value of  $k$  for clinical beams over the range 5 to 30 MeV.<sup>84</sup>

An estimation of the value of  $k$  can be obtained from broad-beam depth dose data obtained earlier for radiation processing of materials.<sup>17</sup> Over the range 1 to 10 MeV, the half-value depth  $R_{50}$  in water varied from 0.31 to 3.77 g/cm with a  $k$  value varying from 3.23 to 2.65, respectively. Over the range 3 to 7

MeV, the half-value depth varied from 0.92 to 2.6 g/cm<sup>2</sup> with a k value varying from 3.26 to 2.69, respectively. More experimental data are needed to establish the behavior of the coefficient k for clinical TSET beams in the energy range for  $1 \text{ MeV} \leq E_0 \leq 10 \text{ MeV}$ . Lillicrap, et al. have found good agreement in using measured narrow beam (2.5 mm diameter) data to construct broad beam distributions over the energy range 4-10 MeV.<sup>74</sup>

#### 6.4 Multiple-field measurements

Two centers have examined the effects on dose distribution of combining various numbers and configurations of treatment fields using cylindrical and other shaped phantoms.<sup>13,43</sup> The effect of beam angulation on central axis depth dose has been studied by Riggs for 4 to 29 MeV electrons used in intraoral and intraoperative radiotherapy. Many electrons entering the skin surface are incident at large angles from the normal to the treatment plane, and the skin surface itself is often significantly curved and oblique to this plane. As a consequence, dose distributions over the patient's skin vary widely, the relative simplicity of small field dose distributions is lost and no simple generalizations are applicable. However, since the radius of curvature of most surface anatomy is large compared to the range of TSET electrons, the depth dose normal to the surface is determined to a large extent by the angle between the incident electron path and the normal to the skin surface. Composite depth dose and isodose curves can be constructed and estimated for regions with large radii of curvature by applying this principle to the contributing fields and then summing and normalizing them.

Bjarngard, et al.<sup>13</sup> have studied the depth dose at various angles of incidence for single and multiple fields at 4 and 7 MeV with 15 cm and 30 cm diameter circular phantoms, as well as with anthropomorphic phantoms, at three meters distance. As the angle of incidence increases, the dose shifts to shallower depths. For large angles it decreases from the surface monotonically with depth, and this shift occurs more rapidly for the lower (4 MeV) energy. They determined the minimum and maximum composite depth doses along radii of cylindrical phantoms for combinations of two, four, six, and eight single fields directed normal to the axis of the cylindrical phantom. For increasing numbers of fields, the dose over the phantom surface becomes more uniform, the dose maximum moves towards the surface and at 4 MeV, the depth-dose curve decreases monotonically from the surface. This is also seen in the data of Figs. 3b and 3c. The mean effective energy  $E_s$ , at the treatment plane for the electron beams contributing to the solid depth-dose curve of Fig. 3c, is estimated to be 1.9 MeV and 3.0 MeV for the dashed curve. Hence, higher electron energies are needed to treat with acceptable uniformity to a given depth with an increased number of fields. Although measurements and calculations were restricted to a transverse plane of the phantom containing the central axis of the beams, extension to planes not containing the



central axis of the beam is feasible. An obvious extension of multiple field treatment is rotation therapy about a vertical axis of the patient.<sup>71,94,109</sup>

### 6.5 Calibration point dose measurements

It is recommended that TSET absorbed dose be evaluated at the calibration point located at (0,0,0) as shown in Fig. 1a. This dose is called the calibration point dose. This is to be carried out using the Bragg-Gray type procedure described in the AAPM TG-21 Protocol using data for electron of energy  $E_0$  determined from  $R_{50}$  as discussed in Section 6.3.<sup>1</sup> Some data for energies below 5 MeV may be found in ICRU Report 35 and the TG-21 Protocol.<sup>1,53</sup> A polystyrene parallel-plate ionization chamber, preferably with a gap of 1 mm or less, and having an established  $N_{90}$  value is used in a polystyrene phantom. Except for the National Bureau of Standards, calibration laboratories do not, at the time of writing, calibrate parallel-plate chambers.  $N_{90}$  for these chambers can be obtained from a comparison with calibrated cylindrical chambers in a photon beam or in an electron beam as described in the TG-21 Protocol. The proximal surface of the cavity is to be placed at the depth of dose maximum using overlying polystyrene. The air volume of the chamber is surrounded by polystyrene to at least 1 cm to the rear, and 5 cm radially. A single dual-field exposure will be employed with the beam axis directed above and below the center of the chamber. No modification of the 5-MeV absorbed dose calibration is made for the megavoltage X-ray contributions to the prescribed patient treatment dose, as described in Section 6.6.

A description of absorbed-dose measurement methodology has been given by Holt, et al., and others.<sup>1,42,49</sup> Since the chamber volume is usually small, the effect of extra-cameral volumes can lead to significant error. A method of testing parallel-plate chambers for this effect has been described.<sup>117</sup> The HPA have recently revised their code of practice for electron beam dosimetry in radiotherapy.<sup>50</sup> They have retained the dose conversion factor,  $C_e$ , used in earlier codes of practice. They recommend a thin-window, parallel-plate chamber for low-energy electron dosimetry and have retained the procedural aspects of their earlier Report Series No. 13 for low-energy electrons.<sup>49</sup> Fricke or other chemical dosimeters may be used to confirm the ionometric absorbed-dose calibration of the treatment beam.

### 6.6 Treatment skin dose measurements

Patient and radiation field asymmetries result in a complicated variation in dose to local anatomical areas in TSET, and no single specification of treatment dose can take cognizance of this variation which may differ from facility to facility. Hence, detailed measurement at all relevant points in the treatment field(s) of TSET patients is a prerequisite for each facility and the effect of this variation on the treatment of individuals and on

comparability must be evaluated.

Despite these limitations, it is desirable to have a single parameter that serves to specify the dose to the patient and which will facilitate the comparison of clinical results with other TSET beams. For this purpose, the treatment skin dose is defined as the mean dose along a circle at or near the surface of a cylindrical polystyrene phantom 30 cm in diameter and 30 cm high which has been irradiated as a hypothetical patient with all six dual fields. This dose lies at or very close to the skin surface and could apply to 4, 6, and 8 dual fields, equally well.

The cylindrical phantom, with appropriate dosimeters attached, usually film or TLD, is exposed with its proximal surface placed in the treatment plane, its cylindrical axis vertical and placed so that its front vertical surface midpoint coincides with the calibration point ( $x = 0$ ,  $y = 0$ , and  $z = 0$ ). as shown in Fig. 1a. Six dual-field exposures, each identical to the single dual-field calibration dose exposure described in Section 6.5, are given with the phantom progressively rotated  $60^\circ$  about its vertical axis between exposures. The dose at  $d_{\max}$  below the phantom surface exhibits a periodicity and has a maximum value every  $60^\circ$  coinciding with the six angular phantom orientations intersecting the plane containing the two beam axes of each dual-field. Because of dose contributions to these maxima from the other five exposures, primarily the two dual fields  $\pm 60^\circ$  on either side, the six maxima occur at shallower depths than for a single dual-field exposure; possibly at the surface of the phantom (see Figs. 3b and 3c). The treatment skin dose has been defined as the mean dose in soft tissue evaluated along the circle passing through these six dose maxima. The dosimeter used for this averaging process is calibrated with a single dual field using the identical exposure at the calibration point as described in Section 6.5.

This enables the calibration point dose to be related to the treatment skin dose by multiplication with a factor B. The electron monitor may be set so that the calibration-point dose is one centigray per monitor unit for the normal dual-field exposure. If D Gy is given for each of six dual fields (0.5 with the machine pointing up and 0.5 with the machine pointing down), the average skin dose given during a complete six-dual-field treatment cycle is  $B \times D$  Gy. Typically, B is the range 2.5 to 3.1 for the example described but is difficult to determine with precision. It results from significant dose contributions from three dual fields and small contributions from others. The uncertainty in this factor, and thus in the mean skin dose determination, should be assessed and stressed to the responsible clinician. A sample treatment prescription is given in Table II.

## 6.7 Precautions and routine checks

A number of precautions and routine checks can serve to

establish confidence in the TSET technique and ensure safety in carrying it out. Many items will be part of an ongoing Quality Assurance program.<sup>106</sup>

It is strongly recommended that a local, written, dated procedure be provided for changing from conventional modalities to TSET and vice versa. This written procedure should be as simple possible and conveniently available at the console. The technologists and physicists involved with TSET should be thoroughly familiar with the changeover procedure and cognizant of normal operating conditions before initiating treatment. The change-over procedure itself, which will depend on local conditions, should be unambiguous and should provide adequate safety interlock confirmation and procedural checks. It should lend itself to rapid execution, preferably taking five minutes or less to carry out. The treatment unit should be "run up" prior to treatment to verify normal operating parameters and monitor operation. A sample change-over procedure is given in Table III.

The extent of participation of the responsible physicist in the change-over will vary from center to center and is a matter of judgment. It depends upon the technique selected, the equipment available to carry it out, experience acquired in using it, the safety features provided, and the training and experience of the technologists involved.

In addition to the redundancy necessary in the dose monitoring system, it is also important to have redundant methods to verify the absorbed dose calibration, especially during the development phase. In vivo dosimetry, such as with small 1 mm<sup>3</sup> TLD chips is recommended for each patient in different regions of the anatomy for at least one treatment cycle. This is particularly important for the first few patients treated after implementation of the technique. Many centers employ daily therapy record forms of different colors depending on treatment modality: brachytherapy, orthovoltage, megavoltage X-rays, small-field electrons, TSET, etc. The color-coding provides instant identification of the modality used and contributes to safety.

## 7. PATIENT CONSIDERATIONS

Many TSET patients are elderly and will prefer high therapy-room temperatures for their comfort when disrobed for treatment.

### 7.1 Patient positioning

Patient alignment is less stringent than for small field modalities, but transverse centering on the beam axis may be conveniently aided with laser alignment lights.

The dosimetry for patients having TSET is often explored using

cylindrical or elliptical-shaped phantoms. The patient presents difficulties in practice because of the self-shielding by the limbs. Therefore, one of the important steps in TSET is to position the patient so as to minimize the areas of self-shielding as shown in Fig. 1c. Usually, there will still be a need for boost fields at normal SSDs. The positions chosen for the arms and legs may vary depending on the number of fields used. The use of six fields or more is recommended.<sup>13,43,102</sup> There may be circumstances when fewer than six fields are used. D'Angio<sup>23</sup> suggests one approach to positioning for a four-field technique, and Smedal<sup>102</sup> another. Occasionally, a small region will be treated with a single dual field and auxiliary shielding. In this situation, the factor B is eliminated in the expression for the treatment skin dose, the  $D_{\max}$  may be below the surface, and the beam is significantly more penetrating than for the full six-dual-field technique.

For the six-dual-field technique, a number of positions can be chosen for the arms and legs. The objective is to minimize self-shielding. For the four oblique fields, the patient can assume a "stride" position so as to expose the upper-medial thighs better. Representative patient body, arm, and leg positions for treatment are illustrated in Fig. 1c for the six-field technique.<sup>91</sup> Similar positions were adapted by Fraass, et al.<sup>27</sup> who have the patient stand on a rotatable base having angle markings and with positions for location of the feet indicated. Such features can improve the accuracy and speed of the setup. A modified "stride" position could be used for the four oblique fields whereby one leg is elevated about 30 cm off the floor on a pedestal so as to expose slightly more of the upper medial thighs. If it is desired to expose the axillary regions slightly more, the arms can be extended upward with the fingers on suitably located straps suspended from supports above the patient.

Kumar, et al.<sup>71</sup> use a cage-type device, motorized to give 5 rev/min for a patient rotation technique. In this case, the patient can grip two of the vertical support rods with arms elevated. This arrangement offers speed and simplicity for daily setups.

Podgorsak, et al.<sup>94</sup> use rotational treatment and have the patient hold on with one arm to a rotatable bar attached to the ceiling with the other arm placed alongside the body. The positions of the two arms are alternated from one treatment to the next.

## 7.2 Patient support devices

It is always prudent to provide some support and allow for a rest period during treatment. For those patients who are able to stand, some judgment is required as to whether some form of auxiliary support is necessary, such as a thin, wide fabric belt

placed around the chest and under the arms. This belt can be attached to the wall or to part of the framework that may be used to support the energy degrader or to support the hand straps above the patient. It is necessary to consider the possibility of a patient becoming weak and fainting. Often patients will be wearing eye shields which tend to cause a loss of orientation. Also, unless told to relax part of the time, they may stand rigidly in the position prescribed. If they stand straight with knees "locked," they are more likely to feel faint after several minutes. The patient should be encouraged to move slightly so as to maintain some degree of relaxation without compromising the treatment position. Since there is always some danger of a patient's falling during the course of a treatment, the room should be equipped with a pan-and-tilt type of TV camera for constant monitoring. The patient should be instructed and encouraged to signal when a need for a rest period is felt.

Typically, a daily TSET session of three dual-field treatments requires 20-25 minutes of facility time. Although a daily treatment skin dose of 1 Gy at a dose rate of 0.25 Gy/min involves only 12 min of beam-on time per day, the sequential patient and machine set up procedures are time consuming (see Section 6.6). Dose rates at the patient of 1.0 or more Gy/min at the calibration point are desirable in reducing treatment times.

Some patients may have difficulty standing for prolonged periods. Ideally, they would be treated best lying on the floor. In this case, the patient could be moved along while lying on a motorized couch and drawn under a narrow transverse beam in the manner described by Trump, et al.<sup>113</sup> However, the equipment for accomplishing this is not generally available unless custom designed and constructed. Patients who clearly cannot manage to stand during the treatment may be treated lying on the floor or on a low stretcher using two or three fields anterior and posterior. This generally implies extended distances such that a beam-defining cone is not used. The electron beam field edges are not well defined in this technique so that materials such as lead rubber will be needed in suitable thicknesses to define the field edges and to avoid overlap of fields. The need for supplementary lateral exposures and abutment doses at field edges can be assessed by film or TLD measurements. Some positioning and monitoring aids for lying patients have been described by Bagne and Tulloh.<sup>6</sup>

The skin of many patients undergoing TSET is very susceptible to damage by scraping and bruising. As a result, attention should be given to eliminating sharp edges that can come in contact with the patients, or against which they may fall. Since the soles of the feet sometimes have cracked and bleeding lesions, it is appropriate to supply disposable bath mats for walking and standing or, alternatively, disposable slippers.

If there is any type of a "cage" in which the patient stands,

especially a portable one, it should be attached securely to the wall or floor to prevent tipping. Depending on the patient positioning, overhead straps for the hands may be required and some means will be needed for support of the straps. To allow for faster positioning, templates can be used to indicate the placement of the feet preferably on Styrofoam or a low bench to reduce scatter from the floor.

### 7.3 Patient shielding

The lens of the eyes will generally be shielded. If the eyelids are to be treated, internal shields placed under the lids must be employed. Other body parts such as the finger nails and toe nails may be shielded by shaped sheet lead when these portions of the anatomy can be safely excluded from the treatment. Depending on clinical involvement and technique, shields for the hands or feet usually have to be provided well before the full course of therapy is completed,

One should be aware of the increased dose to the inner surface of the eyelid, as large at 50%, from the backscatter off the internal high-Z lead eye shield.<sup>28, 35, 65, 68, 79, 88, 99</sup> shielding parts of the anatomy, the shields should be placed near the patient, rather than at the machine collimator. The projected light-field edge is not usable for defining the outer edges of the radiation field at these extended distances due to the multi-directional nature of the widely scattered beam reaching the patient. However, once the angulation of the treatment unit is established, it can be set easily using fiducial marks and the edges of the light-field edge in a darkened room.

Internal eye shields are available commercially but can be made if facilities are available, as suggested by Fraass.<sup>27</sup> A commonly used thickness at 4 MeV is 2.0 mm of lead. Commercial eye shields may provide marginal shielding, depending on the incident electron energy. Eye shields used internally cannot be made as thick as one would prefer. They are likely to offer less protection near the edges where they are thinner, and the transmission there can be in the range of 15% to 25%. If a tab is provided to make insertion easier, there will be an added weight, and the eye shields may have a tendency to slip downward when the patient stands. If the eye shields have sufficiently long tabs, a piece of fabric with a slit for the tab of the eye shield, together with a Velcro head strap, can be used effectively to keep the eye shield centered or, alternatively, tape criss-crossed over each eye.

Eye drops providing a local anesthetic are helpful for insertion of the eye shields. Eye shields need to be kept clean, sterile and free of roughness. They can be stored in 1:1000 Merthiolate and washed after each use with warm water. Mineral oil can be used as a lubricant when the shields are placed in the eye.

A common practice is to keep eye shields coated with paraffin. Other equally effective approaches may be followed in caring for eye shields.

As treatment progresses, various skin reactions are to be expected. Smedal, et al.<sup>102</sup> have listed some of these reactions along with the time sequence for their occurrence. The loss of hair, finger nails and toe nails (if not shielded) is to be expected when the dose exceeds about 10 Gy. The skin may become erythematous, and there may be swelling of feet, ankles, and hands. The radiotherapist may elect to shield those parts of the anatomy for a number of treatments or to halt treatments for one to two weeks. The "red-man" syndrome refers to patients who present with total skin erythroderma. Since no two TSET installations are identical, the shielding thickness requirements should be measured for conditions relevant to actual patient treatment at each facility. These measurements should be repeated if the technique (energy, scatterer, degrader, angle, etc.) is changed.

#### 7.4 Local boost fields

The extent of the area of the boost fields needed will require clinical judgment from the radiotherapist based on the underdosed regions resulting from TSET treatments. These will not be clearly defined regions, as a rule. The areas generally boosted will be the soles of the feet, the perineal area, the dorsal surface of the penis, the skin in the peri-anal region, and the inframammary region in females with large breasts.<sup>70</sup> In the latter case, the use of a thin brassiere during treatment may eliminate the need for boost in that region. In addition, boost fields have been considered necessary for the top of the head and the ear canal in some situations. Frequently, areas to be boosted have already received some dose from the main treatment. Such is the case for the top of the head and to a lesser extent, the inframammary region. In these areas, it is important to know the previously delivered dose distribution so as to not cause a serious over or under dose when delivering the boost field. Boost fields are provided either with conventional electrons, or low-voltage X-rays at customary SSDs. In vivo TLD dose measurements can identify areas requiring local boost fields.

The choice of whether to use electrons or X-rays for boost fields appears not to be based on any clear clinical advantage that one has over the other. In some cases, the decision to use low-voltage X-ray from an orthovoltage or other low-voltage machine may be made because such a unit is readily available and the electron-producing machine may have a heavy patient load. Depending on the HVL of the X-ray beam available, one would probably choose 100 kV or a higher kilovoltage for boost fields. Using electron boosts, one is assured of confining the dose delivered to superficial tissue. However, self-shielding due to skin folds in some patients can present difficulties in boost field

treatment as for TSET.

### 7.5 In Vivo dose measurements

In vivo dosimetry measurements are important for TSET for two reasons: 1) determination of the distribution of dose to the patient's skin, and 2) verifying that the prescribed dose to the patient's skin is correct. Measurements of the dose and the dose distribution with a small phantom at the patient treatment position have been described in several publications.<sup>27,59,62,91,93</sup> The actual uniformity of the dose delivered to the patient's skin, however, may vary significantly from that measured in air, so measurement of the actual skin-dose distribution is required.

Several types of dosimeters may be considered for use in these measurements, including small ionization chambers, diodes, film, and thermoluminescent dosimeters (TLD). However, when one considers the number of areas which should be measured on each patient (at least 40, if one is investigating a new technique), ion chambers and diodes become impractical.<sup>27,92</sup> The use of film is questionable because a rather large number of small film packets or large sheets or strips of film must be used to obtain the requisite data. Since the film and its lightproof packaging are rather thick, one must be concerned about possible interference with the dose that the patient's skin receives. In addition, the problem of eliminating air spaces between the film, film packet, and patient are nontrivial.<sup>77</sup> Thermoluminescent dosimeters, therefore, are the logical choice for in vivo dosimetry for these low-energy electron fields. Studies have shown that TLDs calibrated with <sup>60</sup>Co may differ by about 10% from TLDs calibrated with 4 MeV electrons in a polystyrene phantom.<sup>46</sup> Hence, calibration of TLD with a parallel-plate ion chamber and electrons at TSET energy is recommended. The accuracy of the TLD dose data is adequate for patient dosimetry, since the day-to-day and patient-to-patient variation are much greater than the  $\pm 5\%$  accuracy that can be obtained with careful TLD dosimetry procedures.<sup>27,92</sup> It is important to use the same electron beam for calibrating TLDs for TSET dosimetry, and to use the same chips for calibration and for in vivo patient dosimetry.

A large number of skin-dose measurements have been reported by Fraass, et al.<sup>27,92</sup> using the six-dual-field technique.<sup>59</sup> The results from the study are indicative of the results to be expected from examination of other treatment techniques. The dose to various parts of the chest and abdomen varies only a few percent, as predicted by the in-air dose distribution. However, for many other parts of the body, the measured skin doses are more than 20% different from the dose to the anterior of the abdomen, the reference point. In particular, most parts of the foot and ankle, except the arch, receive between 10% and 25% more dose than the reference point, as do the ears, nose, and fingers. Many areas receive at least 20% less dose than the reference point, including



the forehead and scalp, wrist and palm, axilla, elbow, and medial thigh. The direction and magnitude of most of these nonuniformities have a similar pattern from patient-to-patient, suggesting that the variations are not technique dependent, but rather depend on gross anatomical properties that are more or less the same for all patients.

The results of the study of skin dose uniformity must be used with discretion. Low-dose areas may, in fact, be beneficial to the patient. For example, although the dose to the wrists and palms is only about 75% of the dose to the anterior abdomen, lateral flattening of the beam may not be desirable. Patients may already have reactions to the hand and finger doses,<sup>27</sup> and flattening the beam would increase the dose to that area. Finally, the responses and recurrences of the disease must be correlated with the dose to each area before additional modifications are made to an already complicated treatment technique.

TABLE I. Physical considerations involved in a TSET program,

- |  |                                  |
|--|----------------------------------|
| 1. Treatment field size.               | 6. Prescribed dose               |
| 2. Beam penetration depth.             | 7. Dose rate at treatment plane. |
| 3. Electron energy at treatment plane. | 8. Boost fields.                 |
| 4. Field flatness in treatment plane.  | 9. Patient positioning.          |
| 5. X-ray background.                   | 10. Special patient needs.       |

TABLE II. Mycosis fungoides (MF) TSET treatment prescription. This example prescription is not to be construed as representative of all MF patient treatment prescriptions.

1. Dose - 36 Gy/9 weeks.
2. Fractionation - 4 Gy/week.
  - 4 days/week.
  - 3 dual fields/day.
3. Eyes shielded throughout.
4. Scalp shielded after 25 Gy if no involvement above neck.
5. Protect feet with 20 cm high Pb shield after first 10 Gy when sole boost starts. (Otherwise, 250 kV boost blisters tops of feet.)
6. Boost soles and perineum - Orthovoltage, 100 kV (0.5 Al HVL).
  - After first 10 Gy.
  - Rate, 1 Gy/day.

TABLE III. Changeover procedure for 5 MeV total skin electron therapy. This example is for one particular machine and is not to be construed as applicable to other machines,

1. Set up 5-MeV electron apparatus for LA-3, i.e., ion chamber, jaws, target, modality, key, etc.
2. Set accelerator to "up" angle, 110°.
3. Run 2000 MUs for warm-up. During the run, adjust AFC for maximum rate of output, then adjust PRF knob for 200 MU/min.
4. For calibration, set DOS 1 to 250 MUs and proceed to READY light; Do not turn beam on.
5. Depress toggle in electric channel, calibration box integrator light goes on. (90-second timer starts)
6. Press "BEAM-ON".
7. Note reading on calibration meter after 250 MUs delivered and before 90-second timer runs out. (After 90 s, reading is lost as integrator resets)
8. If the calibration is  $\pm 5\%$  or more out of tolerance, retune AFC, repeat calibration procedure (go to Step 3).
9. If beam fault or abort, and timer light on box is still running, a timer restart may be had by depressing "RESET" toggle on meter box.
10. Do not treat unless calibration is within tolerance.

## BIBLIOGRAPHY

1. AAPM Task Group, Report 21: A protocol for the determination of absorbed dose from high-energy photon and electron beams. Med. Phys. 10:741-771, 1983.
2. ACR, Quality assurance in radiation therapy. A manual for technologists. M.J. Wizenberg, Ed., pp. 171, 1982.
3. Almond, P.R.: Calibration of megavoltage electron radiotherapy beams. In Waggener, Keriakes and Shalek, Eds: Handbook of Medical Physics VI. Boca Raton, Florida, CRC Press 1982, p. 137.
4. Andrews, J.R., Swain, R.W.: The radiation therapy of human cancer with accelerated atomic particles. Med. Ann. of Dist. of Col. XXVI, 13-16, 1957.
5. Asbell, S.O., Siu, J., Lightfoot, D.A., Brady, L.W.: Individualized eye shields for use in electron beam therapy as well as low-energy photon irradiation. Int. J. Rad. Oncol. Biol. Phys. 6:519-521, 1980.
6. Bagne, F. and Tulloh, M.E.: Low energy electrons. In Practical aspects of electron beam treatment planning, AAPM medical physics monograph No. 2. C.G. Orton and F. Bagne Eds. pp. 80-96, 1978.
7. Bagshaw, M.A. and Hoppe, R.T.: Aggressive electron beam therapy for mycosis fungoides: An evolutionary program. In Proceedings of the Symposium on electron beam therapy, F.C.H. Chu and J.S. Laughlin, Eds., 155-163, New York, Sept. 1979.
8. Becker, K: Solid state dosimetry. Cleveland, OH, CRC Press 1973, p. 231.
9. Berger, M.J. and Seltzer, S.M.: Theoretical aspects of electron dosimetry. In Proceedings of the symposium on electron dosimetry and arc therapy, B. Paliwal, Ed., Madison, Sept. 1981, pp. 1-19.
10. Berger, M.J. and Seltzer, S.M.: Tables energy-deposition distributions in water phantoms irradiated by point-monodirectional electron beams with energies from 1 to 60 MeV and applications to broad beams. NBS report, NBSIR 82-2451, 1982.
11. Bewley, D.K.: Collector monitors for electron beams. Phys. Med. Biol. 16:131-133, 1971.
12. Biggs, P.J.: The effect of beam angulation on central axis per cent depth dose for 4-29 MeV electrons. Phys. Med. Biol. 29: 1089-1096, 1984.
13. Bjarngard, B.E., Chen, G.T.Y., Piontek, R.W., Svensson, G.K.: Analysis of dose distributions in whole body superficial electron therapy. Int. J. Radiat. Oncol. Biol. Phys. 2:319-324, 1977.
14. Braams, R.: Superficial radiation therapy of large skin areas. Dermatologica 117:204-214, 1958.
15. Brahme, A., Svensson, H.: Specification of electron beam quality from the central-axis depth absorbed-dose distribution. Med. Phys. 3:95-102, 1976.
16. Brahme, A.: Physics of electron beam penetration: Fluence and

- absorbed dose in Proc. of the symposium on electron dosimetry and arc therapy, Madison, Sept. 1981, pp. 45-68.
17. Brynjolfsson, A.: Three-dimensional dose distribution in samples irradiated by electron beams. In Proceedings of International Conference on radiation research, Radiation Research 14-16, Jan. 1963, Published U.S. Dept. of Commerce, Office of Technical Services. pp. 116-129, 1963.
  18. Buechner, W.W., Van de Graaff, R.J., Burrill, E.A., Sperduto, A.: Thick-target x-ray production in the range from 1250-2350 kilovolts. Phys. Rev. 74:1348-1352, 1948.
  19. Chu, F.C.H., Laughlin, J.S.: Total skin electron beam therapy. In Proceedings of the Symposium on Electron Beam Therapy, New York, Sept. 1979.
  20. Coffey II, C.W., Maruyama, Y., Stewart, B.L., White, G.A.: Electron beam irradiation for mycosis fungoides using variable energy. Reprinted from the Journal of the Kentucky Medical Association, 7 pages. July, 1982.
  21. Conere, T.J., Boag, J.W.: The collection efficiency of an ionization chamber in a pulsed and magnetically swept electron beam: Limits of validity of the two-voltage technique. Med. Phys. 11:465-468, 1984.
  22. Cyr, D.P.: Le Traitement du mycosis fungoides par rayons cathodiques; observations hematologiques. Rev. Belge. Path. et Med. Exper. 24:296-301, 1955.
  23. D'Angio, G.J., Nisce, L.Z., Ho Kim, J.: Weekly total skin electron beam therapy for mycosis fungoides and other cutaneous lymphomata: Further experience. Br. J. Cancer 31(Suppl. II):379-385, 1975.
  24. Dutreix, J., Dutreix, A.: Film dosimetry of high energy electrons. in High-energy radiation therapy dosimetry, J. Laughlin, Ed., Ann. N.Y. Acad. Sci. 161:33-43, 1969.
  25. Edelstein, G.R., Clark, T., Holt, J.G.: Dosimetry for total-body electron-beam therapy in the treatment of mycosis fungoides. Radiology 108:691-694, 1973.
  26. Ekstrand, K.E., Dixon, R.L.: The problem of obliquely incident beams in electron-beam treatment planning. Med. Phys. 9:276-278, 1982.
  27. Fraass, B.A., Roberson, P.L., Glatstein, E.: Whole-skin electron treatment: Patient skin dose distribution. Radiol. 146:811-814, 1983.
  28. Gagnon, W.F., Cundiff, J.H.: Dose enhancement from backscattered radiation at tissue-metal interfaces irradiated with high energy electrons. Br. J. Radiol. 53:466-470, 1980.
  29. Galbraith, D.M., Rawlinson, J.A.: Partial bolussing to improve the depth doses in the surface region of low energy electron beams. Int. J. Radiat. Oncol. Biol. Phys. 10:313-317, 1984.
  30. Galbraith, D.M., Rawlinson, J.A., Munro, P.: Dose errors due to charge storage in electron irradiated plastic phantoms. Med. Phys. 11:197-203, 1984.
  31. Goldie, C.H., Wright, K.A., Anson, J.H., Cloud, R.W., Trump, J.G.: Radiographic properties of X-rays in the two to six million volt range. ASTM Bulletin 201, 49-54, Oct. 1954.

32. Greene, M.H., Dalager, N.A., Lamberg, S.I., Argyropoulos, C.E., and Fraumeni, J.F. Jr.: Mycosis fungoides: Epidemiologic observations. *Cancer Treat. Rep.* 63:597-606, 1979.
33. Grollman, Jr., J.H., Bierman, S.M., Morgan, J.E., Ottoman, R.E.: X-ray contamination in total-skin electron therapy of lymphoma cutis and exfoliative dermatitis. *Radiol.* 85:356-360, 1965.
34. Grollman, Jr., J.H., Bierman, S.M., Ottoman, R.E., Morgan, J.E., Horns, J.: Total-skin electron-beam therapy of lymphoma cutis and generalized psoriasis: Clinical experiences and adverse reactions. *Radiol.* 87:908-915, 1966.
35. Gross, B., Wright, K.A.: Charge distribution and range effects produced by 3 MeV electrons in Plexiglas and aluminum. *Phys. Rev.* 114:725-727, 1959.
36. Hare, H.F., Fromer, J.L., Trump, J.G., Wright, K.A. and Anson, J.H.: Cathode ray treatment for lymphomas involving the skin. *A.M.A. Arch. Derm. and Syphil.* 68:635-642, 1953.
37. Haybittle, J.L.: The protection of multicurie strontium-yttrium (90) sources: *Phys. Med. Biol.* 1:270-276, 1957.
38. Haybittle, J.L.: A 10 curie strontium 90 beta-ray therapy unit. *Br. J. Radiol.* 33:52-54, 1960.
39. Haybittle, J.L.: A 24 curie strontium 90 unit for whole-body superficial irradiation with beta rays. *Br. J. Radiol.* 37:297-301, 1964.
40. Hettinger, G., Svensson, H.: Photographic film for determination of isodose from betatron electron radiation. *Acta Radiol. Ther. Phys.* 5:74, 1967.
- 40a. Ho, A.K., Paliwal, B.R., Attix, F.H.: Charge storage in electron-irradiated phantom material. *Med. Phys.* 13:99-100, 1986.
41. Hogstrom, K.R., Ewton, J.R., Cundiff, J.H., Ames, J.C., McNeese, M.D.: Beam delivery system and dosimetry for total skin electron therapy at MDAH, *Med. Phys.* 11:389, 1984 (abstract).
- 41a. Hogstrom, K.R., Ames, J.C., Cundiff, J.H.: The use of the pencil beam algorithm in designing treatment beams for mycosis fungoides. *Med. Phys.* 10:525, 1983 (abstract).
42. Holt, J.G., Buffa, A., Perry, D.J., Ma, I.C., McDonald, J.C.: Absorbed dose measurements using parallel plate polystyrene ionization chambers in polystyrene phantoms. *Int. J. Radiat. Oncol. Biol. Phys.* 5:2031-2038, 1979.
43. Holt, J.G., Perry, D.J.: Some physical considerations in whole skin electron beam therapy. *Med. Phys.* 9:769-776, 1982.
44. Hoppe, R.T., Fuks, Z., Bagshaw, M.A.: Radiation therapy in the management of cutaneous T-cell lymphomas. *Cancer Treat. Rep.* 63:625-632, 1979.
45. Hoppe, R.T., Cox, R.S., Fuks, Z., Price, N.M., Bagshaw, M.A., Farber, E.M.: Electron-beam therapy for mycosis fungoides: The Stanford University experience. *Cancer Treat. Rep.* 63:691-700, 1979.
46. Horowitz, Y.S.: The theoretical and microdosimetric basis of

- Thermoluminescence and applications to dosimetry. Phys. Med. Biol. 26:765-824, 1981.
47. Horwitz, H., Haybittle, J.L.: Whole body superficial irradiation with strontium 90 beta rays. Br. J. Radiol. 33:440-446, 1960.
  48. HPA: A practical guide to electron dosimetry [5-35 MeV]. The Hospital Physicists' Association, 47 Belgrave Square, London, S.W.1, Report Series No. 4, 1-15, 1971.
  49. HPA: A practical guide to electron dosimetry below 5 MeV for radiotherapy purposes. Hosp. Physicists' Assoc. Report 13:1-18, 1975.
  50. HPA: Code of practice for electron beam dosimetry in radiotherapy. Phys. Med. Biol. 30:1169-1194, 1985.
  51. ICRU Report 21: Radiation dosimetry: Electrons with initial energies between 1 and 50 MeV. International Commission on Radiation Units and Measurements, Maryland, ICRU Publications, 1972, pp. x + 64.
  52. ICRU Report 34: The dosimetry of pulsed radiation. Maryland:ICRU Publications 1982, pp. v + 47.
  53. ICRU Report 35: Radiation dosimetry: Electron beams with energies between 1 and 50 MeV, Maryland: ICRU Publications 1984, pp. x + 157.
  54. Jackson, S.M.: The clinical application of electron beam therapy with energies up to 10 MeV. Br. J. Radiol. 43:431-440, 1970.
  55. Jacobson, A., Birkhead, B., Scott, R.M.: Practical aspects of betatron electron beam dosimetry. Amer. J. Roent. 111:607-612, 1971.
  56. Johnson, T.S., Garciga, C.E., Feldman, M.E., Holcomb, M.H.: Low-megavoltage electron-beam therapy of head and facial skin cancer using a versatile polystyrene collimator system. Radiol. 115:695-699, 1975.
  57. Johnston, D.O., Smedal, M.I., Wright, K.A., Trump, J.G.: Electron beam therapy of widespread superficial malignant lesions: The Surgical Clinics of No. Am. 39:1-6, Lahey Clinic Number, 1959.
  58. Kao, M., Lanzl, L.H., Rozenfeld, M., Kramer, T., Chung-Bin, A.: Electron whole body treatment dose analysis of Stanford technique. Med. Phys. 11:379, 1984 (abstract).
  59. Karzmark, C.J., Loevinger, R., Steele, R.E., Weissbluth, M.: A technique for large-field, superficial electron therapy. Radiology 74:633-644, 1960.
  60. Karzmark, C.J.: Large-field superficial electron therapy with linear accelerators. Br. J. Radiol. 37:302-305, 1964.
  61. Karzmark, C.J.: Some aspects of radiation safety for electron accelerators used for both X-ray and electron therapy. Br. J. Radiol. 40:697-703, 1967.
  62. Karzmark, C.J.: Physical aspects of whole-body superficial therapy with electrons. Front. Radiat. Ther. Oncol. 2:36-54, 1968.
  63. Kepka, A.G., Johnson, P.M., Chicago, Ill. Private communication, 1985.

64. Khan, F.M.: Private communication, 1985.
65. Khan, F.M., Moore, V.C., Levitt, S.H.: Field shaping in electron beam therapy. *Br. J. Radiol.* 49:883-886, 1976.
66. Kim, T.H., Pla, C., Pla, M., Podgorsak, E.B.: Clinical aspects of a rotational total skin electron irradiation. *Br. J. Radiol.* 57:501-506, 1984.
67. Kitagawa, T.: 10 MeV betatron electron beam therapy adapted to a case of mycosis fungoides. *Am. J. Roent. Rad. Therapy & Nuc. Med.* 88:229-234, 1962.
68. Klevenhagen, S.C., Lambert, G.D., Arbabi, A.: Backscattering in electron beam therapy for energies between 3 and 35 MeV. *Phys. Med. Biol.* 27:363-373, 1982.
69. Kumar, P.P., Henschke, U.K., Mandal, K.P., Nibhanupudy, J.R., and Patel, I.S.: Early experience in using an 18 MeV linear accelerator for mycosis fungoides at Howard University Hospital. *J. of Nat'l Med. Assn.* 69:223-227, 1977.
70. Kumar, P.P., Henschke, U.K., Nibhanupudy, J.R.: Problems and solutions in achieving uniform dose distribution in superficial total body electron therapy. *J. Natl. Med. Assoc.* 69:645-647, 1977.
71. Kumar, P.P., Patel, I.S.: Rotation technique for superficial total body electron beam irradiation. *J. Natl. Med. Assoc.* 70:507-509, 1978.
72. Kumar, P.P., Patel, I.S.: Comparison of dose distribution with different techniques of total skin electron beam therapy. *Clinical Radiol* 33:495-497, 1982.
73. Le Bourgeois, J.P., Bridier, A., Bouhnik, H. and Schlienger, M.: Whole cutaneous irradiation in mycosis fungoides with 55 kV x-rays. *Bull. of Cancer* 64:313-322, 1977.
74. Lillicrap, S.C., Wilson, Patricia and Boag, J.W.: Dose distributions in high energy electron beams: Production of broad beam distributions from narrow beam data. *Phys. Med. Biol.* 20:30-38, 1975.
75. Lo, T.C.M., Salzman, F.A., Moschella, S.L., Tolman, E.L., Wright, K.A.: Whole body surface electron irradiation in the treatment of mycosis fungoides. *Radiol.* 130:453-457, 1979.
76. Lo, T.C.M., Salzman, F.A., Costey, G.E., Wright, K.A.: Megavolt electron irradiation for localized mycosis fungoides. *Acta Radiol. Oncol. Radiat. Phys. Biol.* 20:71-74, 1981.
77. Loevinger, R., Karzmark, C.J., Weissbluth, M.: Radiation therapy with high-energy electrons. Part I. Physical considerations 10 to 60 MeV. *Radiol.* 77:906-927, 1961.
78. Marinello, G., Buscaill, A., Baillet, F.: Degradation de l'energie d'un faisceau fixe d'electrons de 7 MeV en vue du traitement du mycosis fongoide. *J. Radiol. Electrol.* 58:693-699, 1977.
79. McGinley, P.H., McLaren, J.R., Barnett, B.R.: Small electron beams in radiation therapy. *Radiol.* 131:231-234, 1979.
80. Meyler, T.S., Blumberg, A.L. and Purser, P.: Total skin electron beam therapy. *Cancer* 42:1171-1176, 1978.
81. Millar, R.M., Coles, J.R., Kenny, M.B.: Whole skin electron beam therapy by rotation. 8-page manuscript. Authors at

- Physical Sciences, Cancer Institute, Peter MacCallum Hospital, Melbourne, Australia.
82. Miller, C.W.: Industrial radiography and the linear accelerator. *J. Br. Inst. Radio Engrs.* 14:361-375, 1954.
  83. Morgan J.E., Dowdy, A.H.: Some problems peculiar to electron therapy. *Radiol.* 81:317-319, 1963.
  84. NACP: Procedures in external radiation therapy dosimetry with electron and photon beams with maximum energies between 1 and 50 MeV. *Acta Radiol. Oncol.* 19:55-79, 1980.
  85. NCRP Report 51: Radiation protection design guidelines for 0.1-100 MeV particle accelerator facilities. 1-159, National Council on Radiation Protection and Measurements, Washington, 1977.
  - 85a. Niroomand-Rad, A., Gillin, M.T., Komaki, R., Kline, R.W., Grimm, D.F.: Dose distribution in total skin electron beam irradiation using the six-field technique. *Int. J. Rad. Oncol., Biol., Phys.* 12:415-419, 1986.
  86. Nisce, L.Z., Safai, B., Poussin-Rosillo, H.: Once weekly total and subtotal skin electron beam therapy for Kaposi's sarcoma. *Cancer* 47:640-644, 1981.
  87. Nisce, L.Z., Safai, B., and Kim, J.H.: Effectiveness of once weekly total skin electron beam therapy in mycosis fungoides and Sezary syndrome. *Cancer* 47:870-876, 1981.
  88. Okumura, Y., Mori, T., Kitagawa, T.: Modification of dose distribution in high-energy electron beam treatment. *Radiol.* 99:683-686, 1971.
  89. Orchard, P.G., Martin-Smith, P.: Surface ionization ratios for electrons in the energy range 3-11 MeV and the implications for treatment of superficial lesions. *Br. J. Radiol.* 44:817, 1971.
  90. Osman, G.E.: Spatial variation of dose and energy in air for 2-6 MeV electron beams. Manuscript consisting of 6 pages, Roswell Park Memorial Institute, Buffalo, NY., 1970.
  91. Page, V., Gardner, A., Karzmark, C.J.: Patient dosimetry in the electron treatment of large superficial lesions. *Radiol.* 94:635-641, 1970.
  92. Palos, B., Fessenden, P.: TL dosimetry for treatment of mycosis fungoides with 4 MeV electrons. *Med. Phys.* 9:618, 1982 (abstract).
  93. Pla, C., Heese, R., Pla, M., Podgorsak, E.B.: Calculation of surface dose in rotational total skin electron irradiation. *Med. Phys.* 11:539-546, 1984.
  94. Podgorsak, E.B., Pla, C., Pla, M., Lefebvre, P.Y., Heese, R.: Physical aspects of a rotational total skin electron irradiation. *Med. Phys.* 10:159-168, 1983.
  95. Proimos, B.S., Wright, K.A., Trump, J.G.: Modification of strontium 90 emission for superficial therapy. *Br. J. Radiol.* 33:640-643, 1960.
  96. Riker, G.: Characteristics of a p-Si detector in high energy electron fields. *Acta. Rad. Oncol.* 24:71-74, 1985.
  97. Sarna, G.P. and Kagan, A.R.: Mycosis fungoides. in *Cancer Treatment*, 2nd Ed., Haskell, C.M., Ed., W. B. Saunders, Philadelphia, 829-835, 1985.



98. Saunders, J.E.: The application of the logarithmic response of silicon diodes to monitoring beam symmetry and electron energy. *Phys. Med. Biol.* 19:373-378, 1974.
99. Saunders, J.E., Peters, V.G.: Back-scattering from metals in superficial therapy with high energy electrons. *Br. J. Radiol.* 47:467-470, 1974.
100. Seltzer, S.M., Hubbell, J.H. and Berger, M.J.: Some theoretical aspects of electron and photon dosimetry. in *Proceedings - IAEA International Symposium on National and International standardization of radiation dosimetry, Atlanta, December 1977*, pp. 3-43, 1978.
101. Sewchand, W., Khan, F.M., Williamson, J.: Total-body superficial electron-beam therapy using a multiple-field pendulum-arc technique. *Radiol.* 130:493-498, 1979.
102. Smedal, M.I., Johnston, D.O., Salzman, F.A., Trump, J.G., Wright, K.A.: Ten year experience with low megavolt electron therapy. *Am. J. Roent. Rad. Ther. & Nuc. Med.* 88:215-228, 1962.
103. Smedal, M.I., Salzman, F., Trump, J.G., Costey, G.C., Wright, K.A.: Clinical safety in low megavolt electron therapy. *Radiol.* 90:370-371, 1968.
104. Spittle, M.F.: Electron-beam therapy in England. *Cancer Treat. Rep.* 63:639-641, 1979.
105. Svensson, H., Hettinger, G.: Dosimetric measurements at the Nordic medical accelerators. I. Characteristics of the radiation beam. *Acta Radiol.* 10:369-384, 1971.
106. Svensson, G.K., et al.: Physical aspects of quality assurance in radiation therapy. *AAPM Report No. 13*, p. 63, 1984.
107. Szur, L., Silvester, J.A., Bewley, D.K.: Treatment of the whole body surface with electrons. *The Lancet*, pp. 1373-1377, June 1962.
108. Tadros, A.A.M., Tapperman, B.S., Hryniuk, W.M., Peters, V.G., Rosenthal, D., Roberts, J.T., Figueredo, A.T.: Total skin electron irradiation for mycosis fungoides: Failure analysis and prognostic factors. *Int. J. Radiat. Oncol. Biol. Phys.* 9:1279-1287, 1983.
109. Tetenes, P.J., Goodwin, P.N.: Comparative study of superficial whole-body radiotherapeutic techniques using a 4-MeV nonangulated electron beam. *Radiol.* 122:219-226, 1977.
110. Thwaites, D.I.: Charge storage effect on dose in insulating phantoms irradiated with electrons. *Phys. Med. Biol.* 29:1153-1155, 1984.
111. Trump, J.G., van de Graaff, R.J., Cloud, R.W.: Cathode rays for radiation therapy. *Am. J. Roentgenol. Radium Therapy & Nuclear Med.* 43:728-734, 1940.
112. Trump, J.G., Wright, K.A., Clarke, A.M.: Distribution of ionization in materials irradiated by two and three million-volt cathode rays. *J. Appl. Phys.* 21:345-348, 1950.
113. Trump, J.G., Wright, K.A., Evans, W.W., Anson, J.H., Hare, H.F., Fromer, J.L., Jacque, G., Horne, K.W.: High energy electrons for the treatment of extensive superficial malignant lesions, *Am. J. Roent., Rad. Ther. & Nuc. Med.* 69:623-629,

- 1953.
114. Wachsmann, F.: Anwendung mittelschneller elektronen in der strahlentherapie. *Strahlentherapie* 139:385-388, 1970.
  115. Weatherburn, H., McMillan, K.T.D., Stedeford, B., Durrant, K.R.: Physical measurements and clinical observations on the backscatter of 10 MeV electrons from lead shielding. *Br. J. Radiol.* 48:229-230, 1975.
  116. Williams, P.C., Hunter, R.D., Jackson, S.M.: Whole body electron therapy in mycosis fungoides--a successful translational technique achieved by modification of an established linear accelerator. *Br. J. Radiol.* 52:302-307, 1979,
  117. Williams, P.C., Jordan, T.J.: Extra-camerol-volume effects in ionization chambers for electron beam dosimetry. *Phys. Med. Biol.* 29:277-279, 1984.
  118. Wright, K.A., Granke, R.C., Trump, J.R.: Physical aspects of megavolt electron therapy. *Radiol.* 67:553-560, 1956.
  119. Wright, K.A., Trump, J.G.: Back-scattering of megavolt electrons from thick targets. *J. Appl. Phys.* 33:687-690, 1962.
  120. Wright, K.A., Trump, J.G., Salzman, F.A., Lo, T., Costey, G.E.: Physical aspects of megavolt electron beam therapy. *Proc. of the Symposium on Electron Beam Therapy*, F.C.H. Chu and J.S. Laughlin, Eds. Memorial Sloan-Kettering Cancer Center (Library of Congress Catalog No. 81-80244), pp. 149-153, Sept. 1981.